Physics and technology in quantum point contacts (QPCs)

Yoshiro Hirayama
NTT Basic Research Laboratories and CREST-JST

1. Fabrication and quantized conductance
2. Effect of confinement potential
3. 0.7 structure
4. Magnetic field dependence
5. Series and multi-parallel QPCs
6. Surface effects
7. Nanoscale understanding of QPCs

QPCs: Quantum point contacts (one-dimensional ballistic channel)

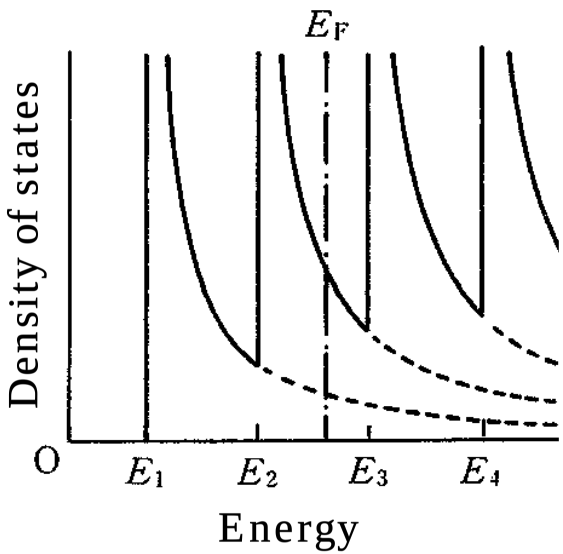

One-dimensional DOS of each subband

$$D_n(E) = \frac{g_s}{h}\sqrt{\frac{m^*}{2(E-E_n)}}$$

Electrons move on fermi surface at T=0

$$E_F - E_n = \frac{1}{2}m^* v^2$$

$$v = \sqrt{\frac{2(E_F - E_n)}{m^*}}$$

Application of small *V*

$$I_n = D_n(E_F)ev(eV) = g_s e^2 V / h$$

Total current = Sum of current of each subband
(*i*;number of subbands under fermi level)

$$I = \sum_{n=1}^{i} I_n = g_s e^2 V i / h$$

change to conductance

$$G = I/V = 2e^2 i / h \quad (g_s = 2)$$

Ballistic mean free path of high mobility 2DEG

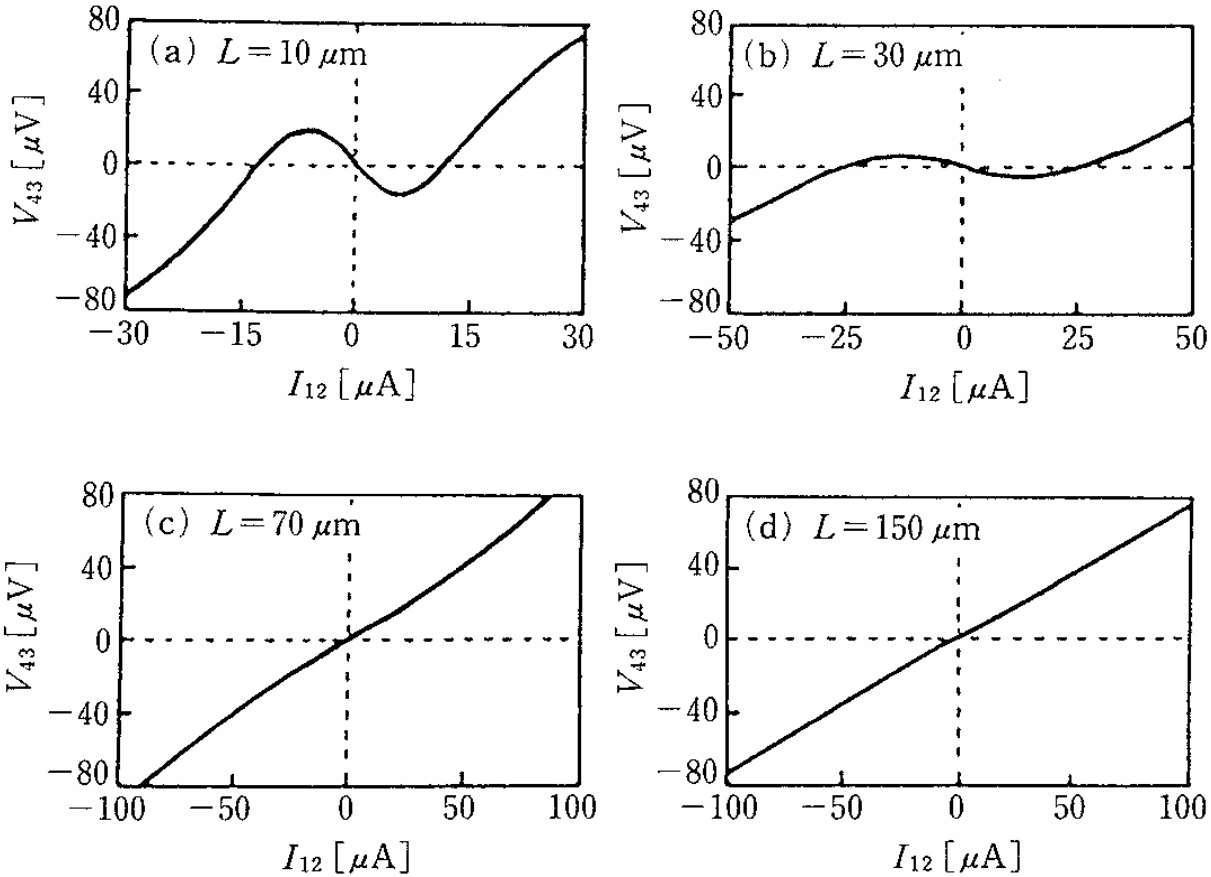

1.5 K

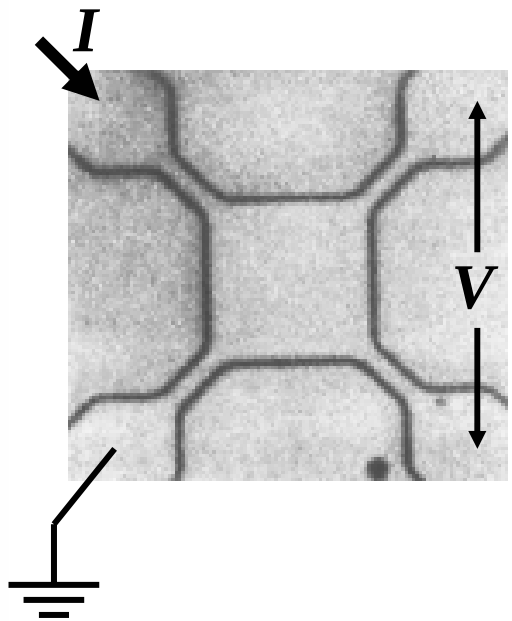

$$le = \frac{h\mu\sqrt{n}}{\sqrt{2\pi e}} \propto \mu, \sqrt{n}$$

l_e ~ 10 μm (n ~ 3x10^{11} cm^{-2}, μ ~ 10^6 cm^2/Vs)

l_e ~ 100 μm (n ~ 3x10^{11} cm^{-2}, μ ~ 10^7 cm^2/Vs)

Hirayama et al., Appl. Phys. Lett. 56, 2672 (1991)

QPCs: Quantum point contacts (one-dimensional ballistic channel)

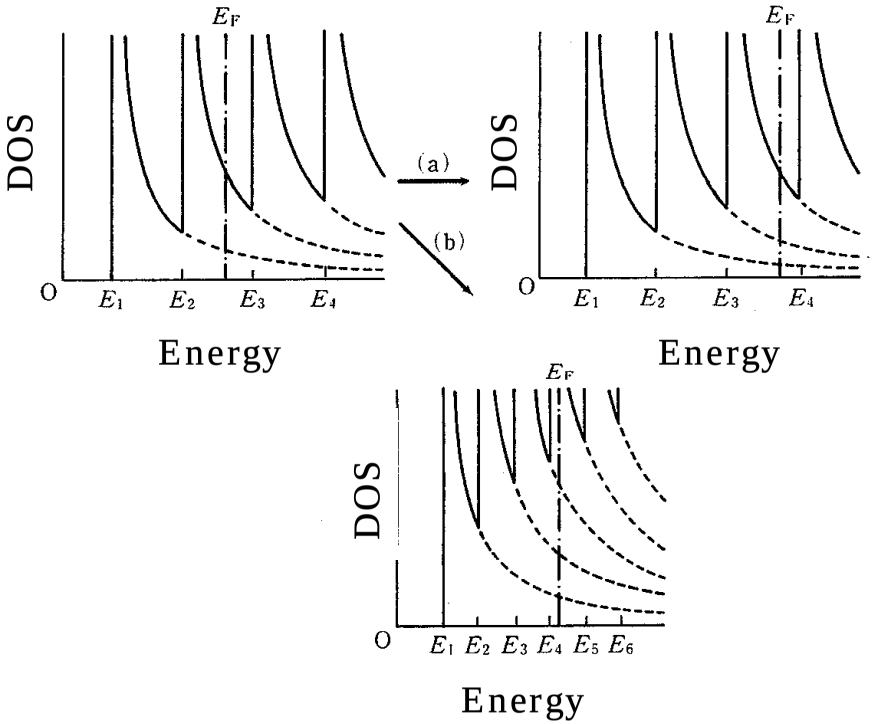

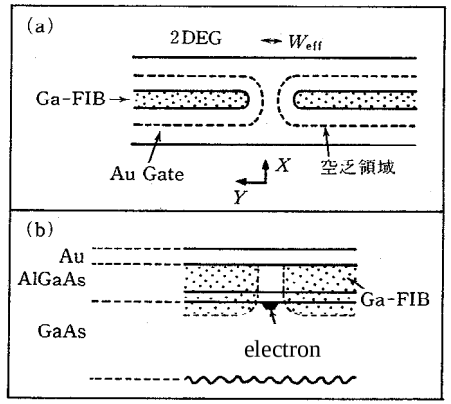

(a)

insulation + gate

width: ~ constant

density: variable

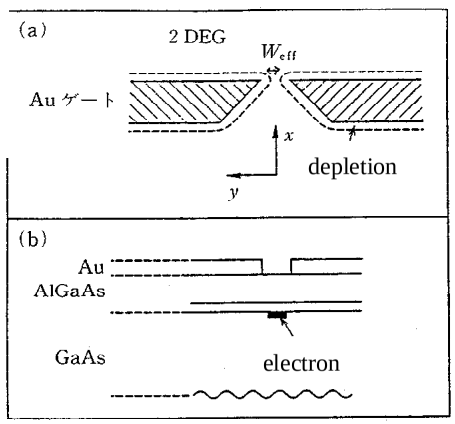

(b)

split-gate or in-plane gate

width: variable

density: ~ constant

Split-Schottky gate QPCs and quantized conductance

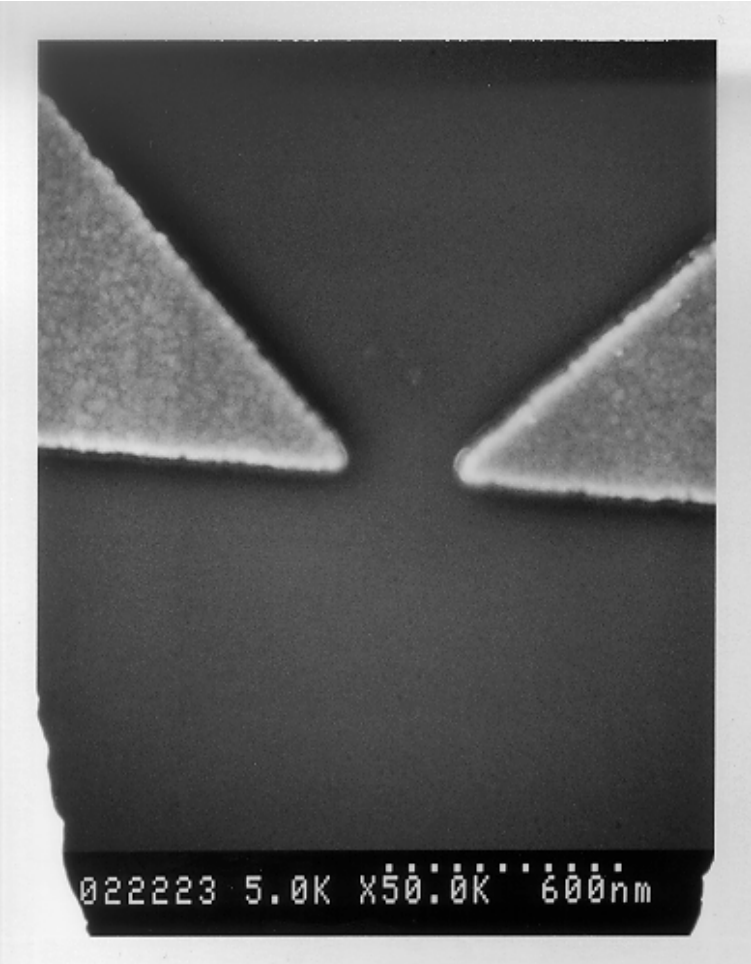

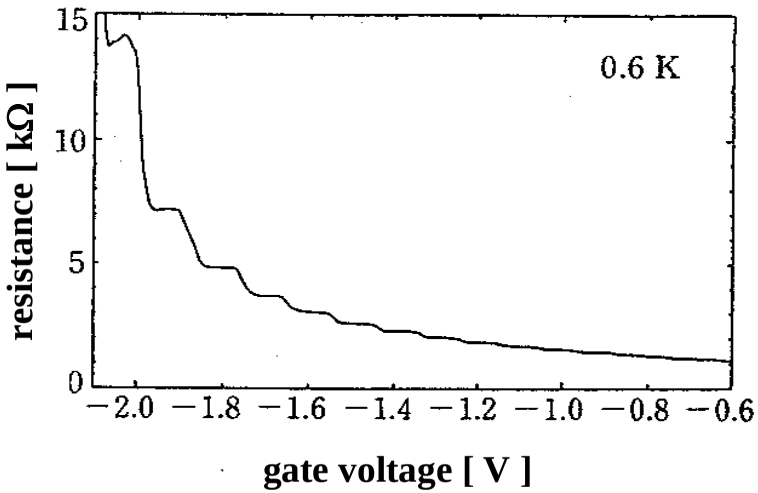

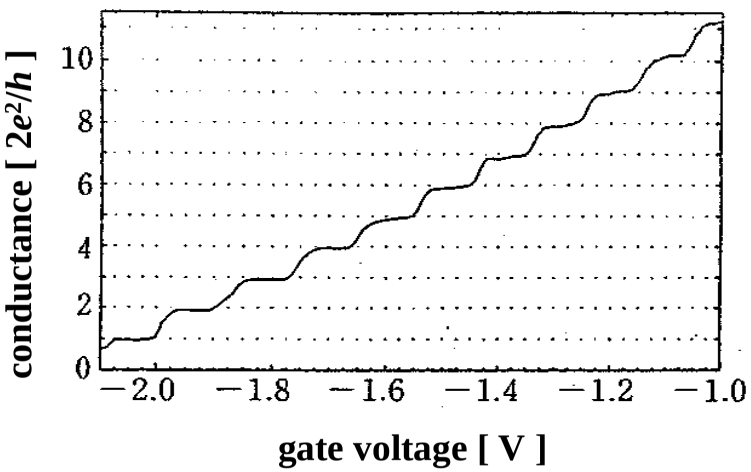

B. J. van Wees et al., Phys. Rev. Lett. 60, 848 (1988)
D. A. Wharam et al., J. Phys. C21, L209 (1988)
and others

Other types of QPCs (in-plane gate QPCs)

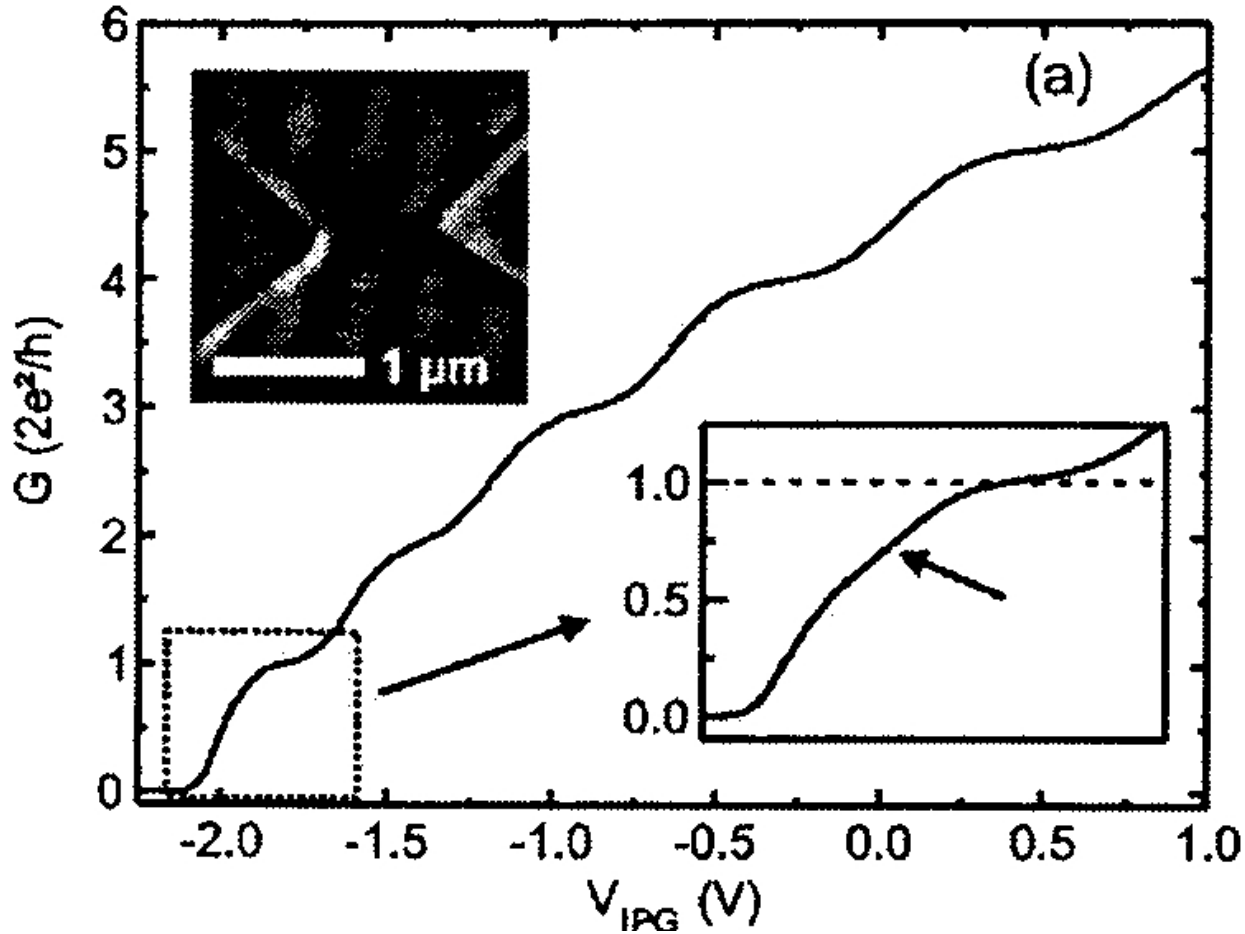

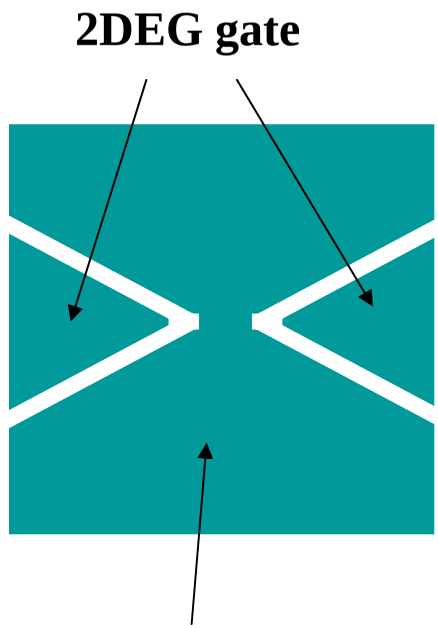

A. D. Wieck and K. Ploog, Appl. Phys. Lett. 56, 928 (1990)

J. Regul *et al.*, Appl. Phys. Lett., 81, 2023 (2002)

Other types of QPCs (focused-ion-beam written QPCs)

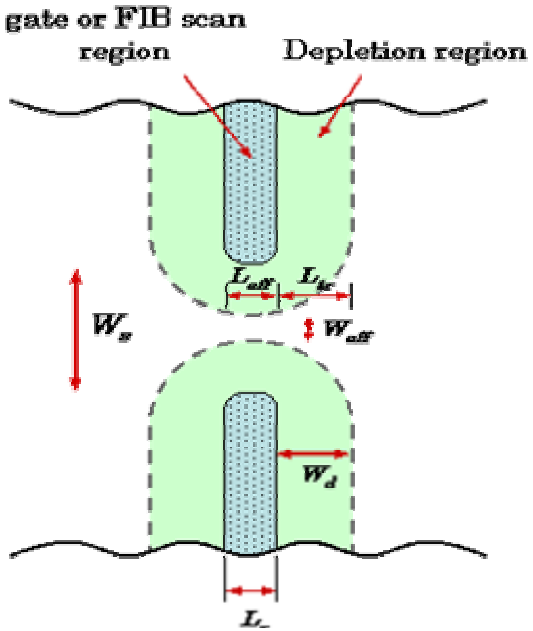

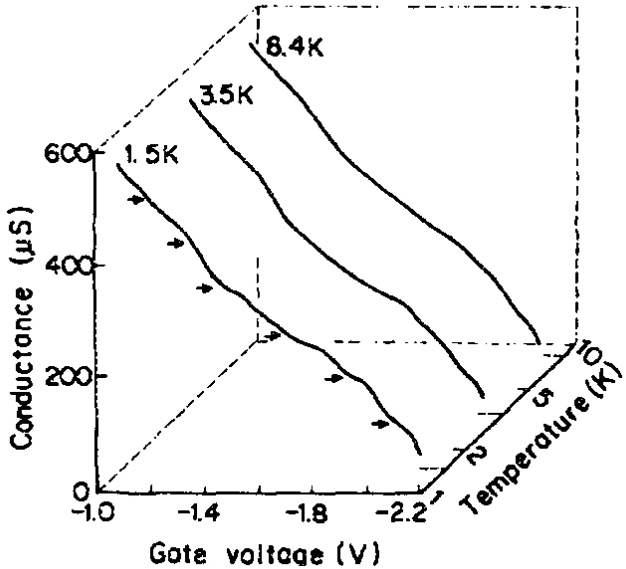

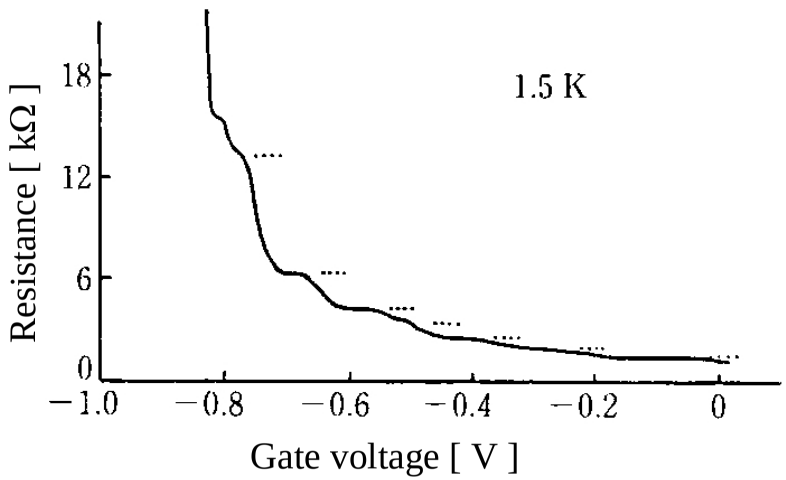

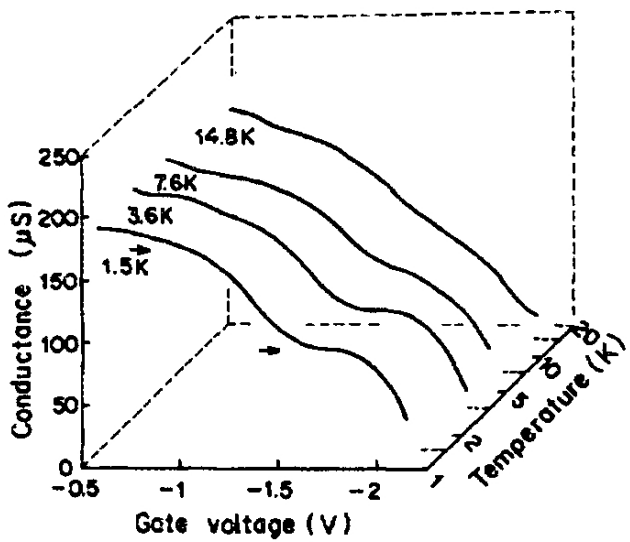

Y. Hirayama and T. Saku, Appl. Phys. Lett., 54, 2556 (1989)

Confinement potential and quantized conductance characteristics
----- reflection of electron wave at both ends ------

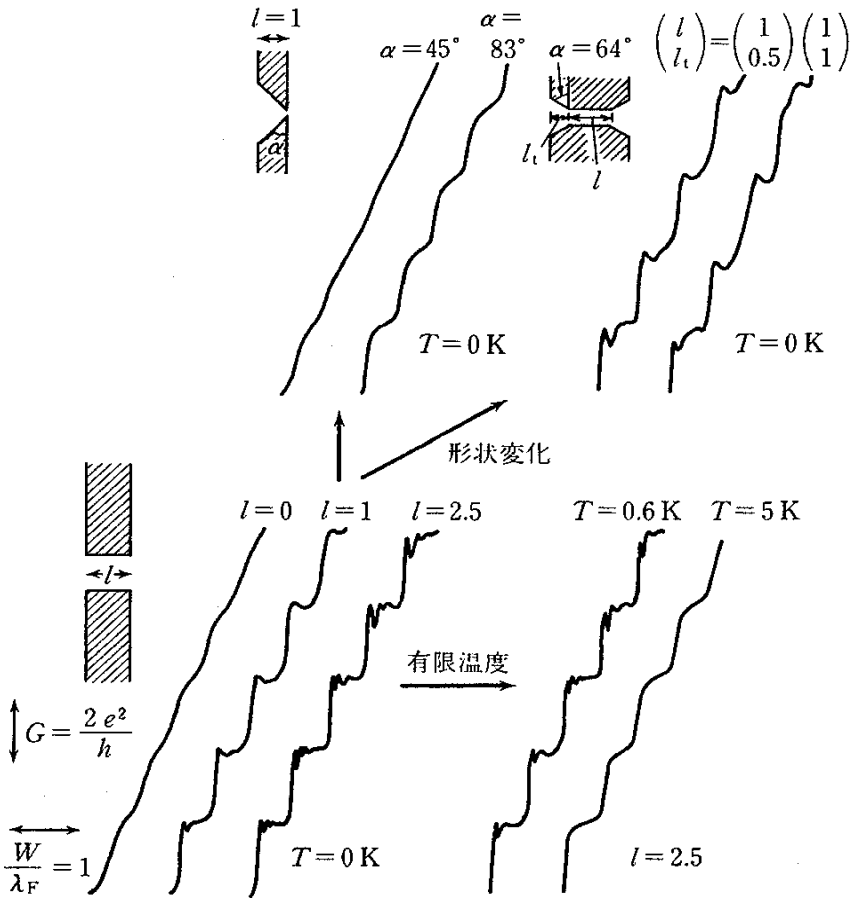

Abrupt width change in a waveguide results in a wave reflection.

Reflected electron wave makes interference and conductance oscillation appears.

Oscillation is determined by λ_{1D} and l_{eff}.

$$2\ell_{eff} = \lambda_{1D} i_r \quad (i_r: \text{ integer})$$

$$\lambda_{1D} = \frac{h}{\sqrt{2m^*(E_F - E_n)}}$$

l is represented by a unit of λ_F

$$\lambda_F = \frac{h}{\sqrt{2m^* E_F}}$$

E. Tekman and S. Ciraci, Phys. Rev. B39, 8772 (1989)
B40, 8559 (1989) theory

Confinement potential and quantized conductance characteristics
----- reflection of electron wave at both ends ------

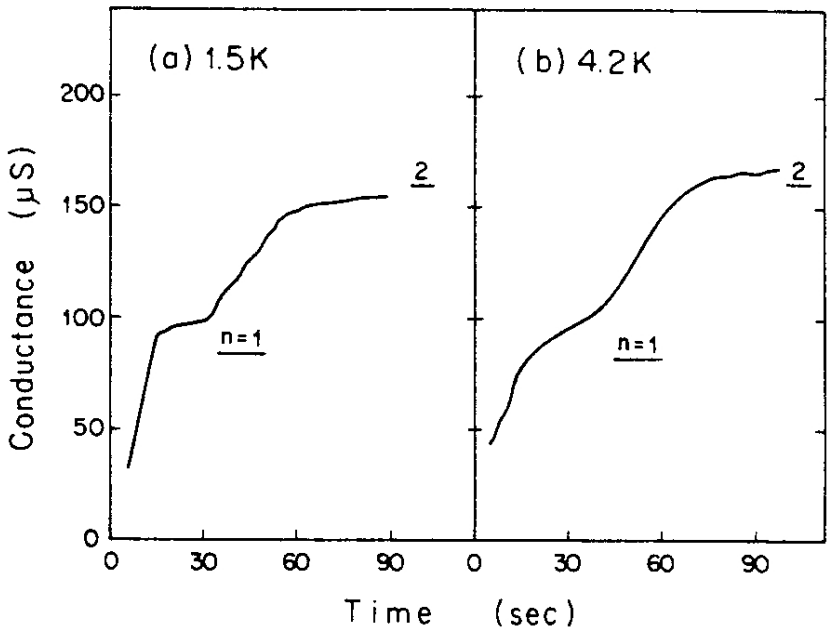

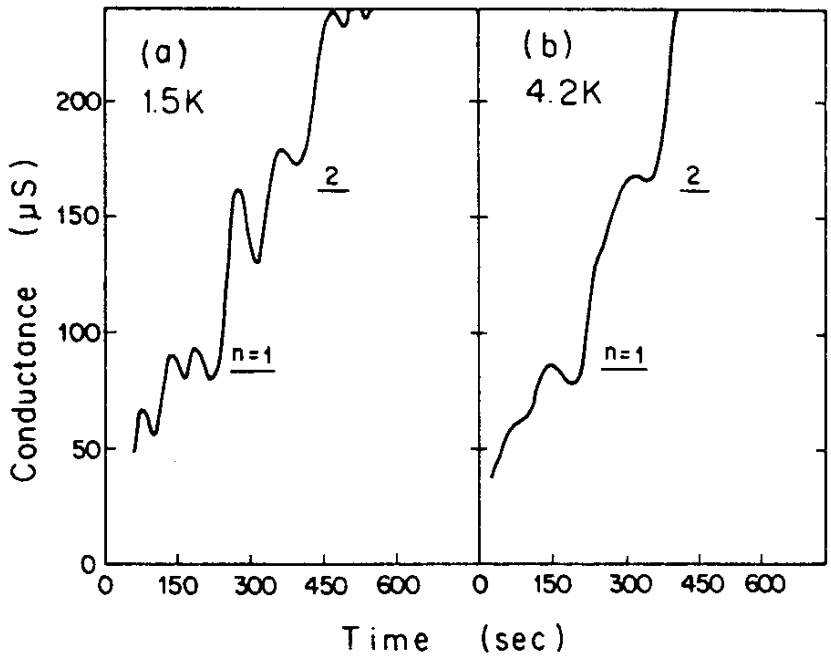

small electron density

↓

large depletion spreading
rounded corner

large electron density

↓

small depletion spreading
sharp corner

Experiments: **Y. Hirayama *et al.*, Jpn. J. Appl. Phys. 28, L701 (1989)**

Quantized conductance characteristics for model potentials

hyperbola boundary $\frac{y^2}{(C\cos\alpha)^2} - \frac{x^2}{(C\sin\alpha)^2} = 1$

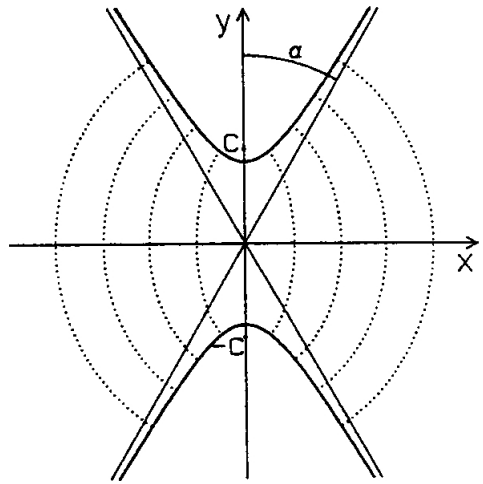

elliptic coordinate

$x = c\sinh u \sin v$

$y = c\cosh u \cos v$

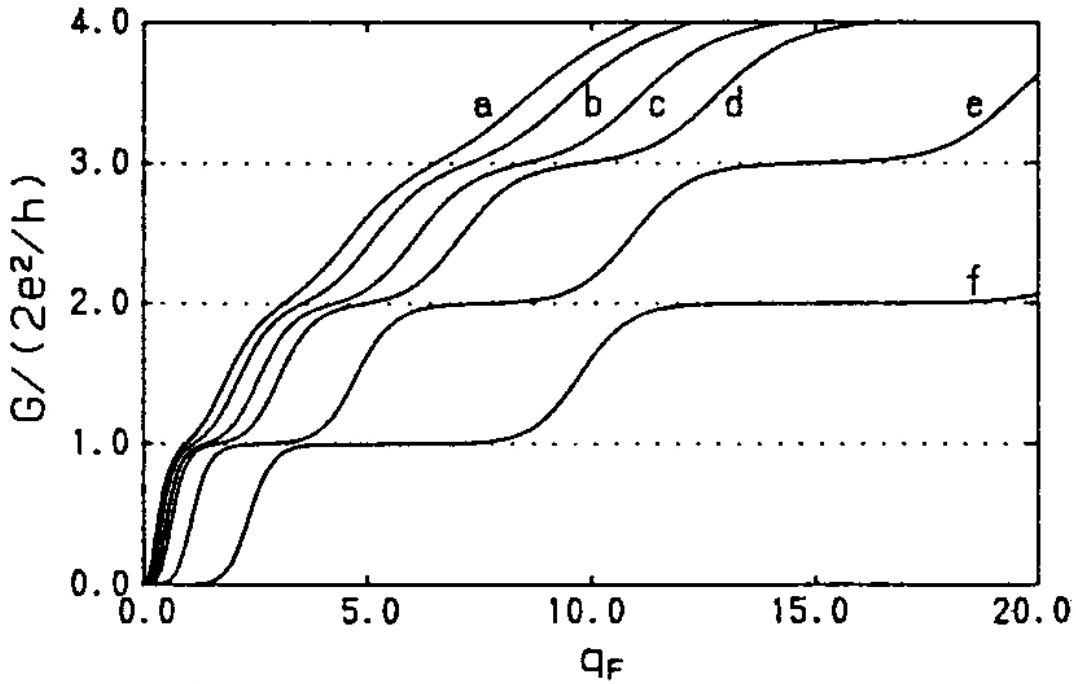

$q_F = \frac{m\varepsilon_F c^2}{2\hbar^2}$

$\alpha = 0, \frac{\pi}{16}, \frac{\pi}{8}, \frac{\pi}{6}, \frac{\pi}{4}$ and $\frac{\pi}{3}$

$(a \to f)$

A. Kawabata, J. Phys. Soc. Japan, 58, 372 (1989)

Quantized conductance characteristics for model potentials

Saddle potential configuration: M. Büttiker, Phys. Rev. B41, 7906 (1990).

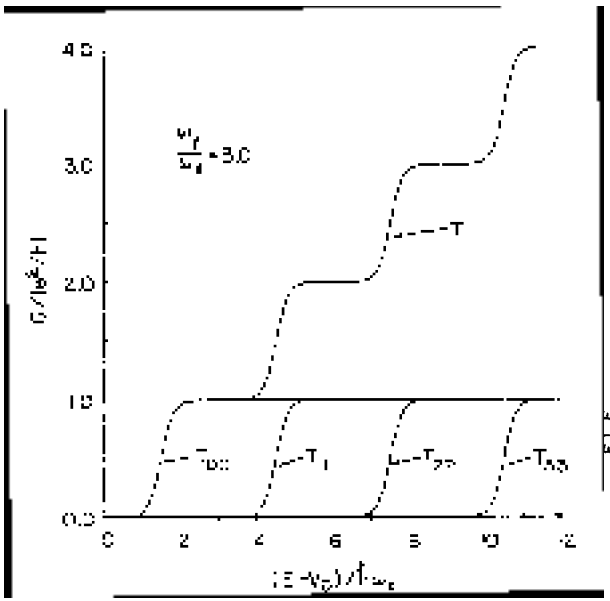

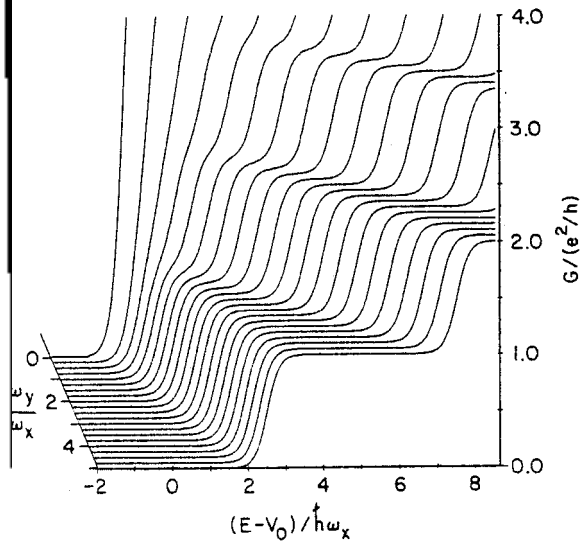

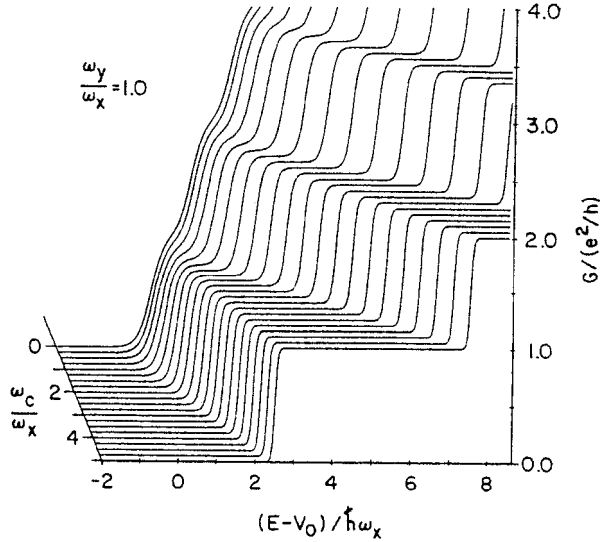

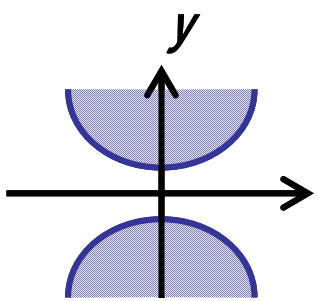

Saddle potential

$$V(x,y) = V_0 - \frac{1}{2}m^*\omega_x{}^2x^2 + \frac{1}{2}m^*\omega_y{}^2y^2$$

Transmission rate of each channel

$$T_n = \frac{1}{1+e^{-\pi\varepsilon_n}} \qquad \varepsilon_n = 2(E - \hbar\omega_y(n+\frac{1}{2}) - V_0)/\hbar\omega_x$$

Total transmission $T = \sum T_n$

Confinement potential and quantized conductance characteristics
----- Backgated QPCs -----

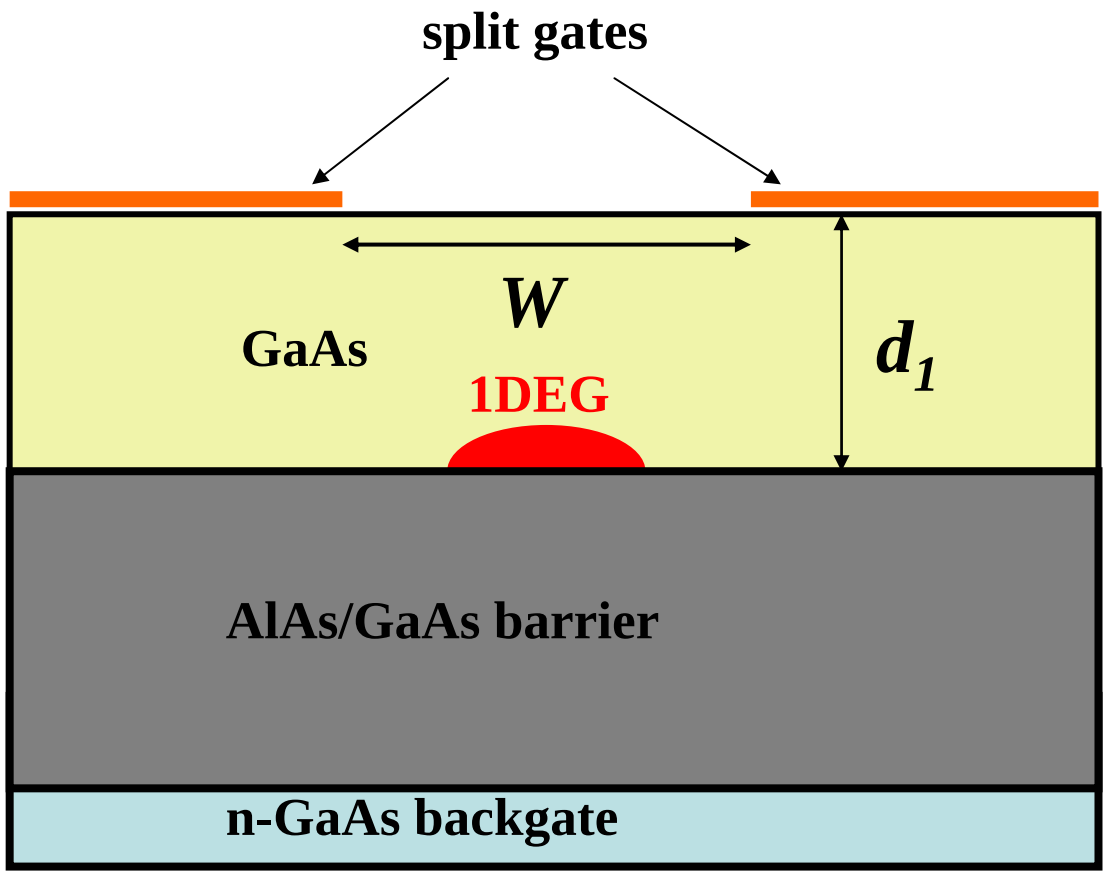

small d_1 (small W)

↓

small ω_x and large ω_y

large d_1 (large W)

↓

large ω_x and small ω_y

Confinement potential and quantized conductance characteristics

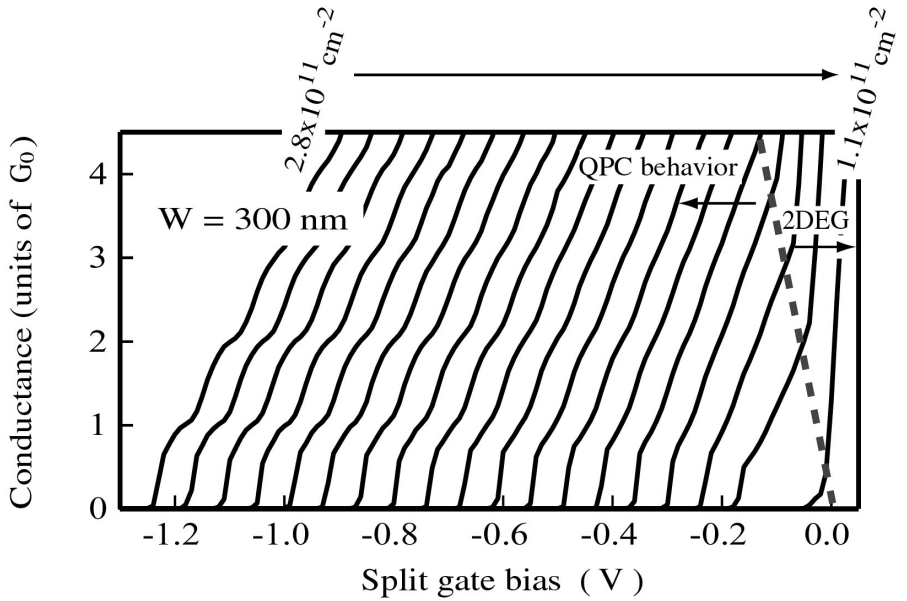

$T = 1.4\text{K}$

$W = 300\text{nm}$, $d_1 = 250\text{nm}$

- Quantized steps become obscure in low-density regions due to a thermal broadening effect.

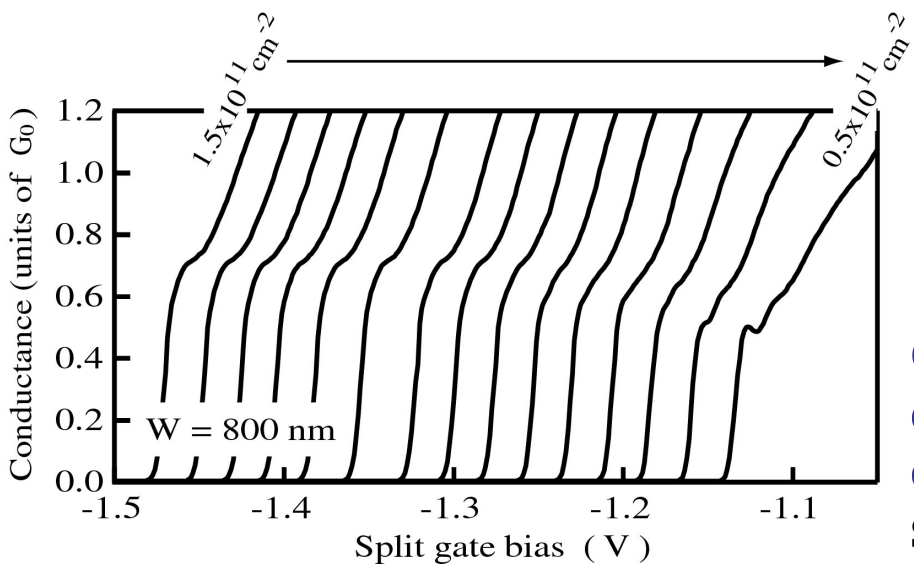

$W = 800\text{nm}$, $d_1 = 500\text{nm}$

- Quantized steps are obscure even in high-density regions and at very low temperature due to the confinement potential effect.
- The 0.7 structure clearly remains.

Conductance of the anomalous plateau drops to around $0.5G_0$ when the electron density decreases.

S.Nuttinck et al., JJAP39, L655 (2000)

Backgated Quantum Point Contact at 100 mK

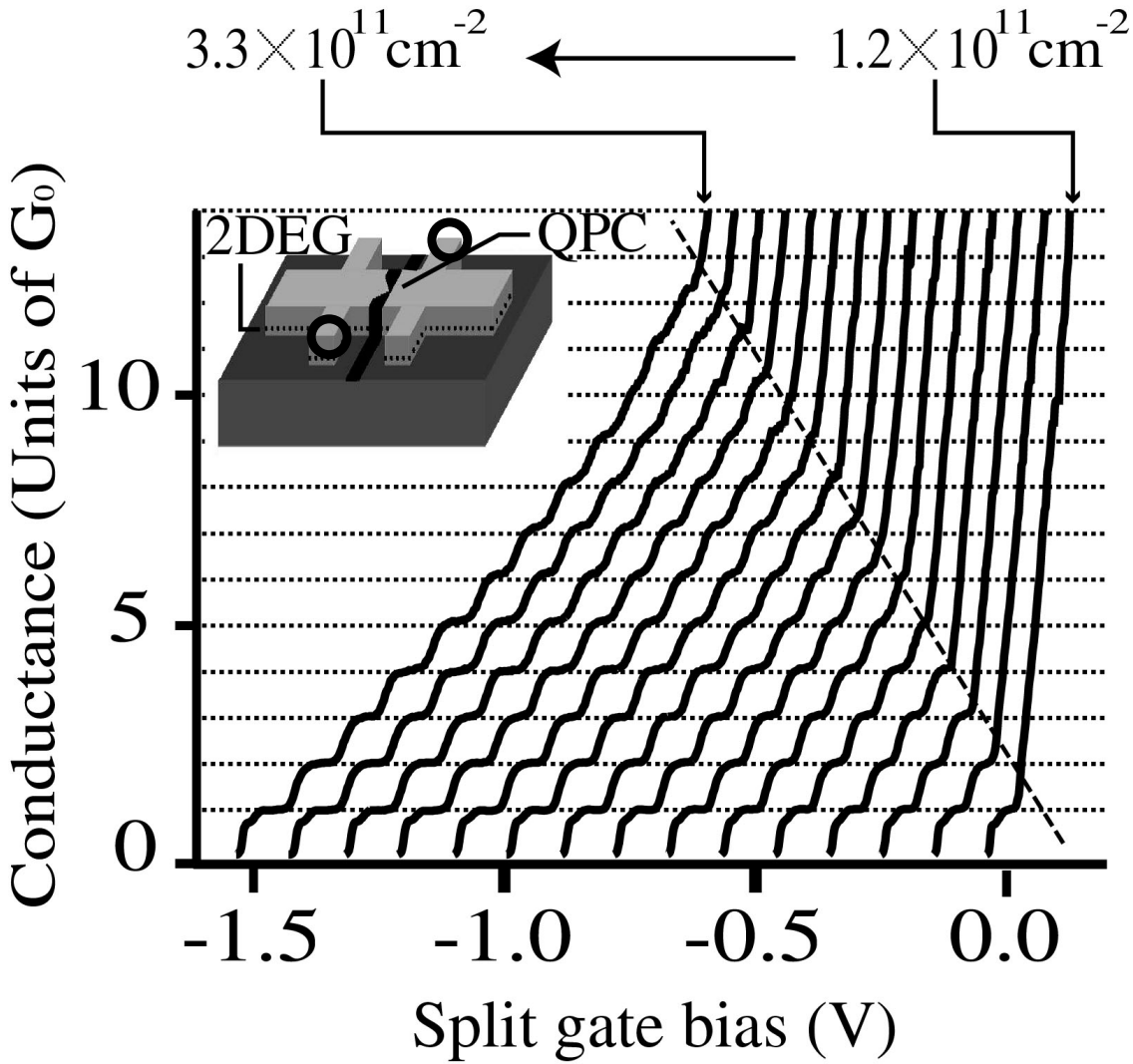

W = 300nm

d_1 = 250nm

100mk

V_b : 1 → 2.4V (0.1V/step)

electron density:

1.2 x 10^{11} → 3.3 x 10^{11} cm^{-2}

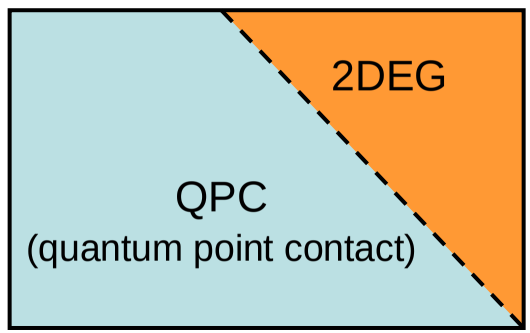

$$G_0 = \frac{2e^2}{h}$$

K. Hashimoto *et al.*, Jpn. J. Appl. Phys., 40, 3000 (2001)

Expanded View of the Conductance below 1.2 G_0 at 100 mK

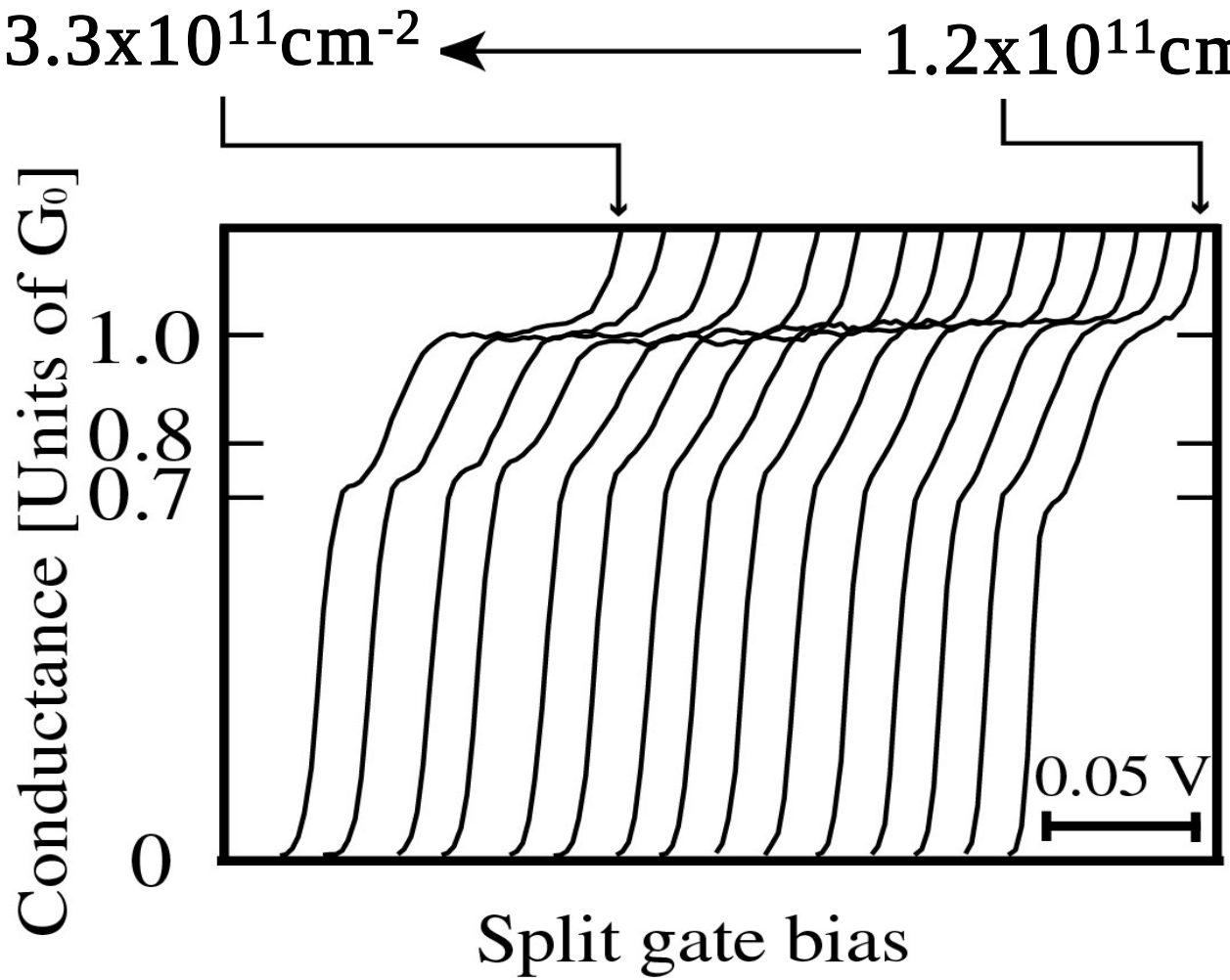

Quantized step:

appear ~ 1.0G_0

- clear step over entire range of densities

0.7 anomaly:

appear 0.68 ~ 0.8G_0

- kink rather than step at around 0.8G_0 for the intermediate electron density (~2 x 10^{11}cm^{-2})
- more apparent step at around 0.7G_0 for both the higher and lower density regions

W = 300nm, d_1 = 250nm

K. Hashimoto *et al.*, Jpn. J. Appl. Phys., 40, 3000 (2001)

0.7 anomaly ---- summary of experiments

0.7 anomaly

*** intrinsic feature related with electron spin**

*** more prominent at higher temperatures**

*** between 0.5 and 0.8, and prominent step at around 0.7**

*** shift to 0.5 under low-electron-density, long-channel, and high-electron-density**

(strong interaction ?)

References K. J. Thomas et al., PRL, 77, 135 (1996); K. J. Thomas et al., PRB58, 4846 (1998), A. Kristensen et al., Physica B249-251, 180 (1998), S.Nuttinck et al., JJAP39, L655 (2000), K. J. Thomas et al., PRB61, R13365 (2000), K. S. Pyshkin et al., PRB62, 12584 (2000), K. Hashimoto et al., JJAP40, 3000 (2001), D. J. Reilly et al., Phys. Rev. B63, 121311 (2001), A. Kristensen and H. Bruus, Physica Scripta (2002), S. M. Cronenwett et al., Phys. Rev. Lett., 88, 226805 (2002)

QPCs made on different materials

Higher temperature operation

Different degeneracy

Spin-orbit interaction

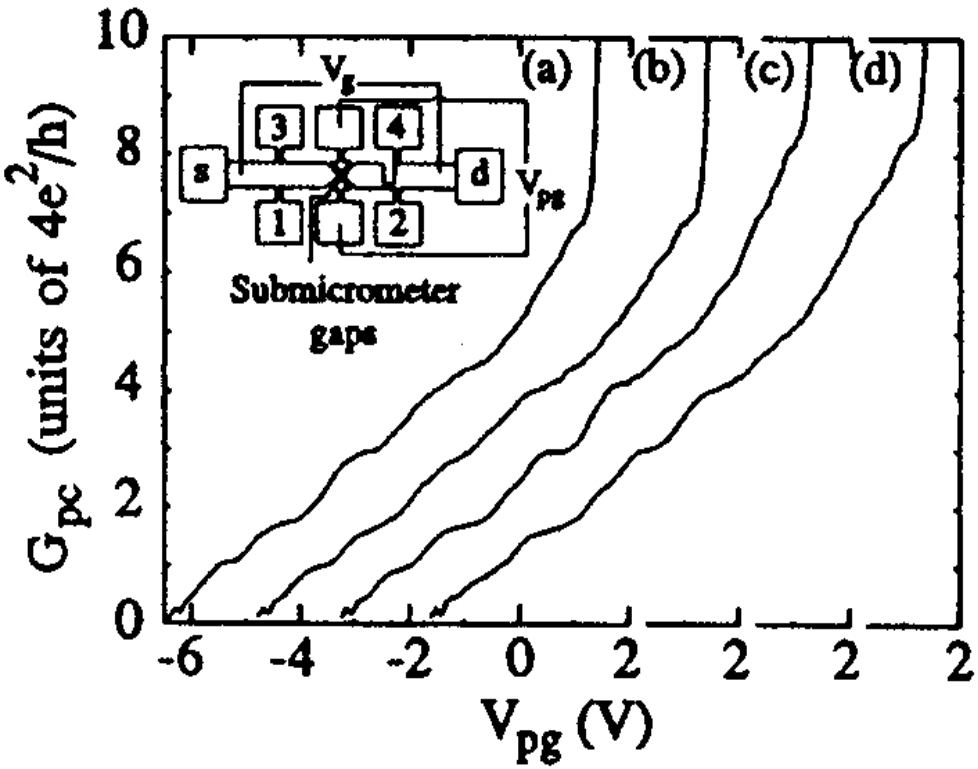

Si: valley degeneracy

2 e^2/h ------> **4** e^2/h

high-mobility Si MOSFET

μ : 2.2x10^{4}cm^2/Vs (n : 5.6x10^{11}cm^{-2})

S. L. Wang et al., Phys. Rev. B46, 12873 (1992)

QPCs made on different materials

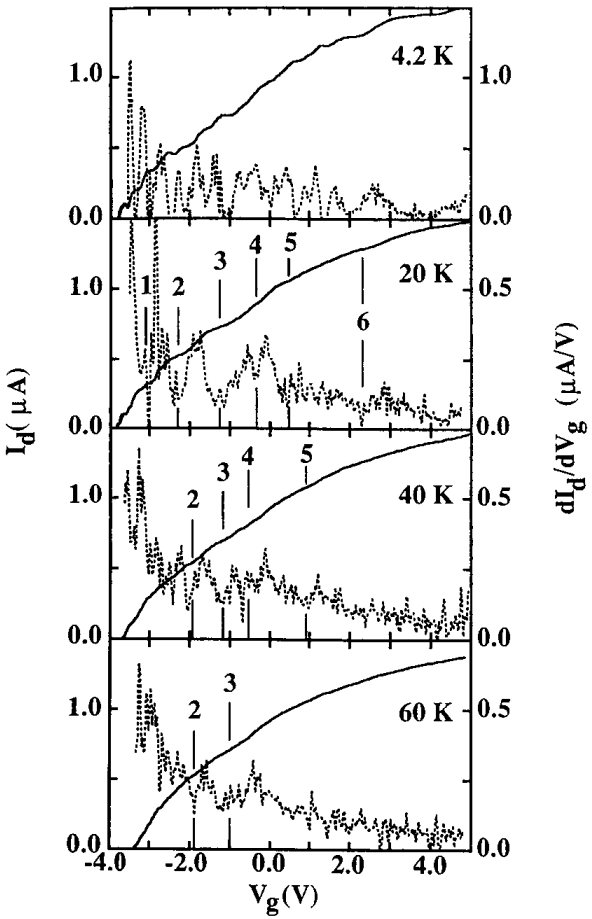

$In_{0.53}Ga_{0.47}As/InAlAs$

in-plane gates (FIB)

T. Bever *et al.*, Jpn. J. Appl. Phys., 33, L800 (1994)

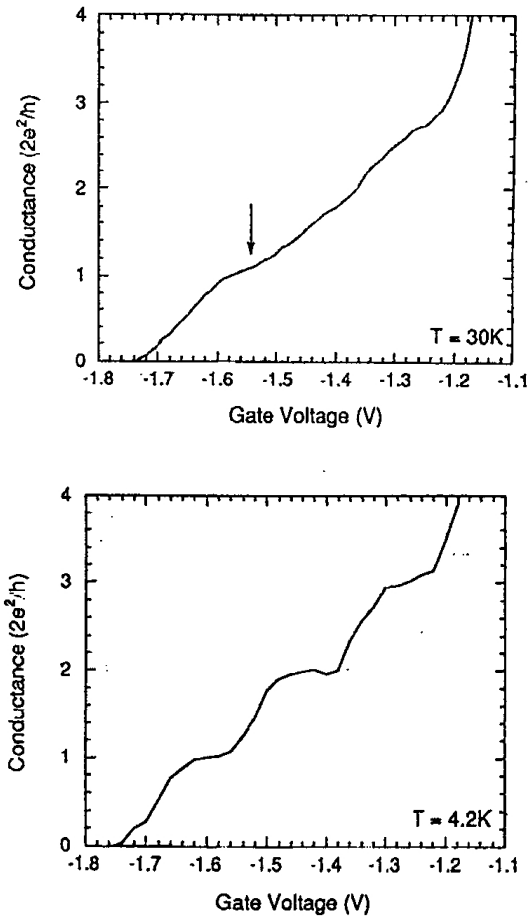

InAs/AlSb **split-gates**

S. J. Koester *et al.*, Appl. Phys. Lett. 62, 1373 (1993)

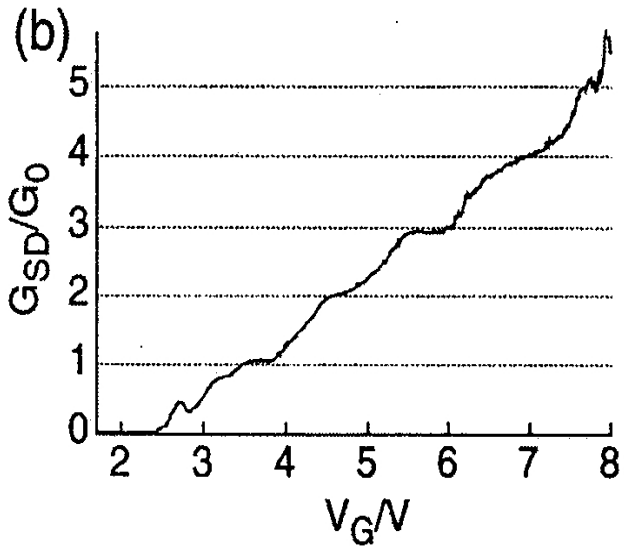

4.2 K

$In_{0.53}Ga_{0.47}As/InP$

in-plane gates

J. J. Westroem *et al.*, Appl. Phys. Lett. 70, 1302 (1997)

Transport characteristics of QPCs
: perpendicular magenetic field dependence

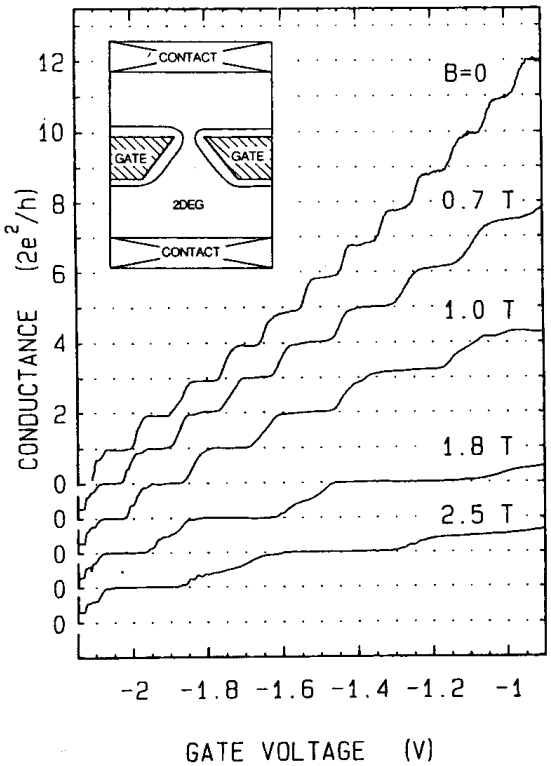

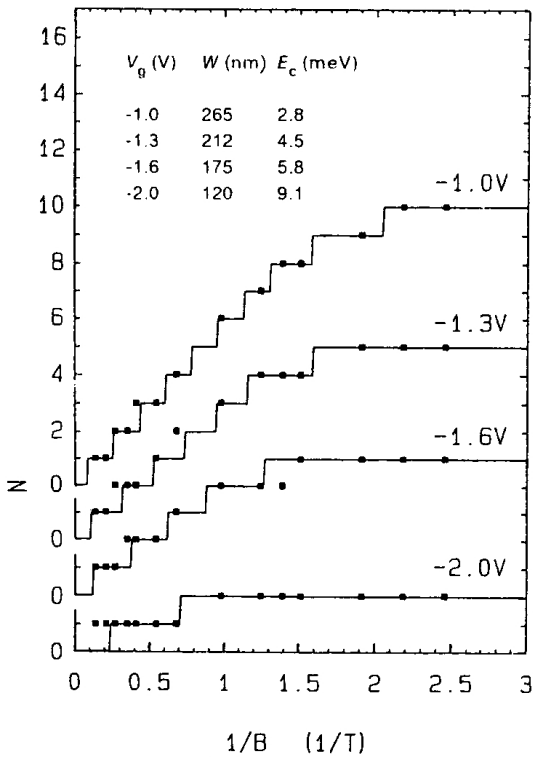

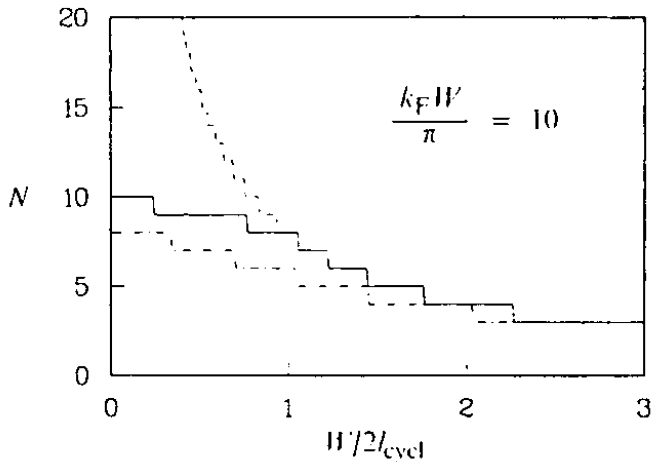

B. J. van Wees *et al.*, Phys. Rev. B38, 3625 (1988).

Depopulation of 1D subband:

$$\hbar\omega_0 \rightarrow \hbar\sqrt{\omega_0^{\,2} + \omega_c^{\,2}}$$ **(1D subband energy separation)**

from QPCs to integer quantum Hall effects

Four-terminal and two-terminal measurements

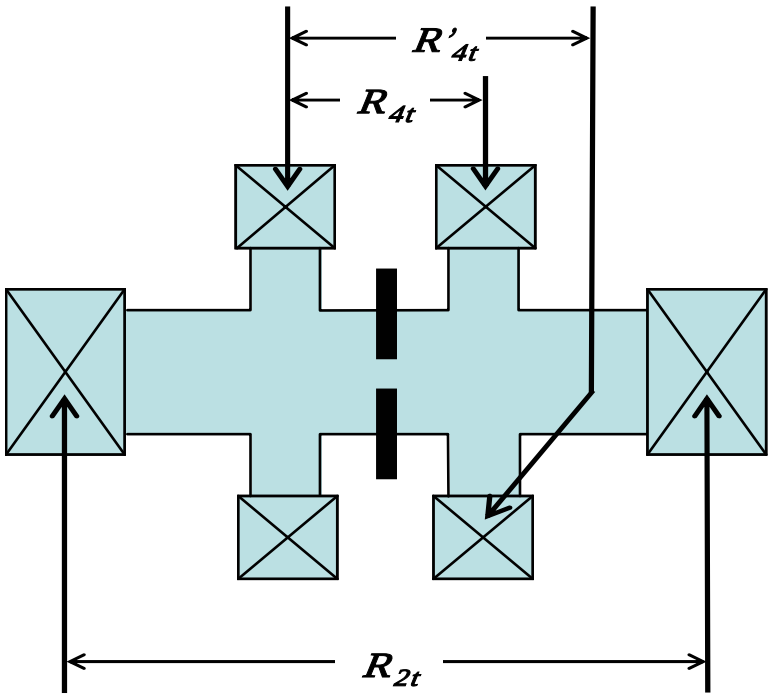

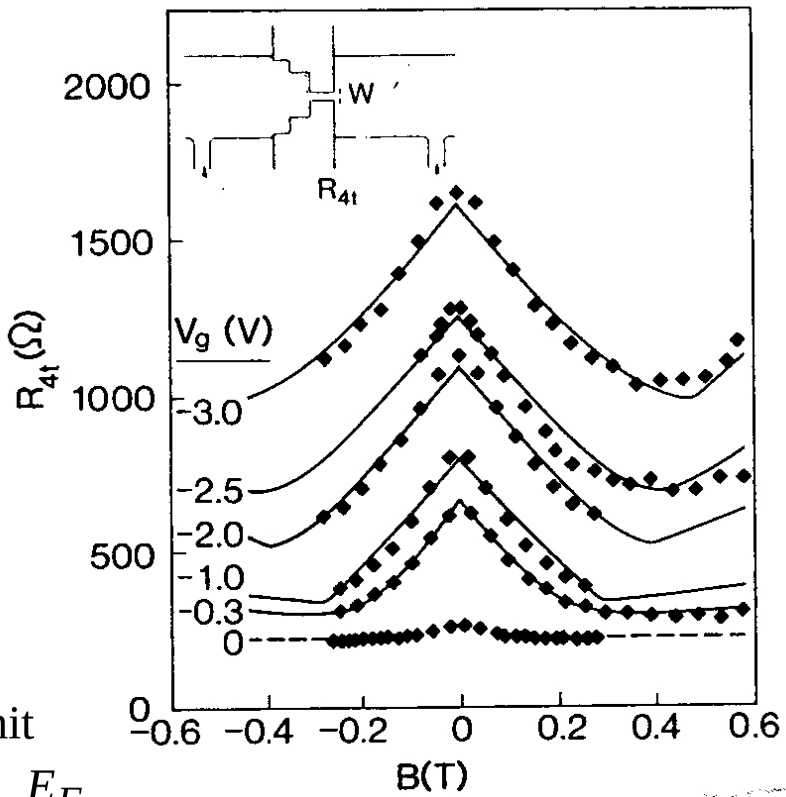

high magnetic field limit

$$R_{4t} = \frac{h}{2e^2}\left(\frac{1}{i} - \frac{1}{i_{wide}}\right)$$

$$i \approx \frac{E_F}{\hbar\sqrt{{\omega_c}^2 + {\omega_o}^2}} \rightarrow \frac{E_F}{\hbar\omega_c}$$

$$i_{wide} \approx \frac{E_F}{\hbar\omega_c}$$

$$R_{2t} = \frac{h}{2e^2}\frac{1}{i}$$

$$R_{2t} = \frac{h}{2e^2}\frac{1}{i} \rightarrow \frac{h}{2e^2}\frac{1}{i_{wide}}$$

H. van Houten *et al.*, Phys. Rev. B37, 8534 (1988).

Series QPCs

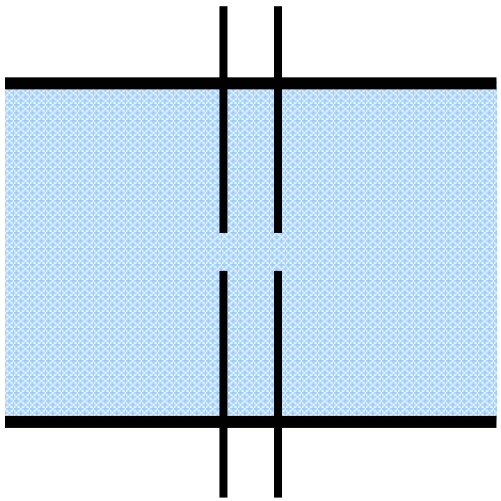

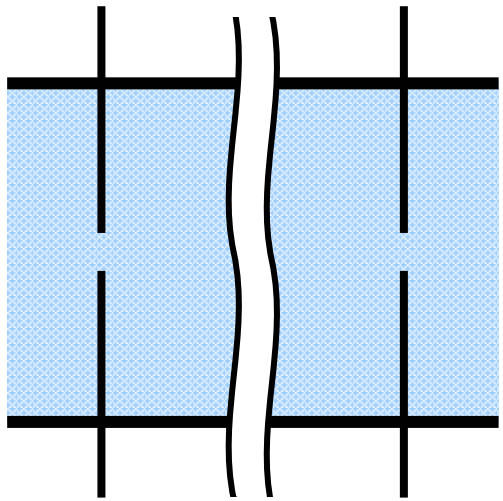

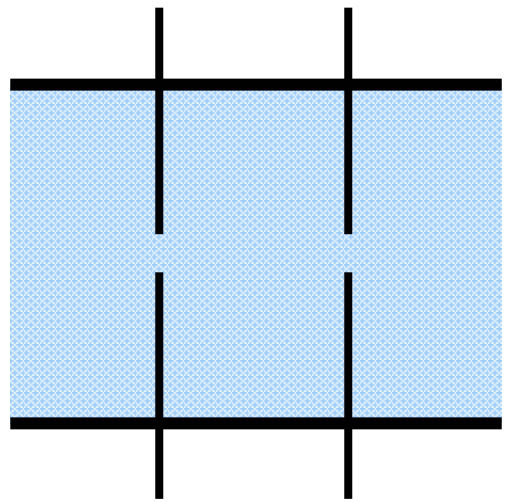

$$R_{total} = R_{QPC}$$

$$= \frac{h}{2e^2}\frac{1}{i}\,(i:\ \text{integer})$$

$$R_{total} = 2R_{QPC}$$

$$= \frac{h}{2e^2}\frac{2}{i}$$

$$R_{QPC} <$$

$$R_{total} = \frac{h}{2e^2}\frac{2}{i+T_d}$$

$$< 2R_{QPC}$$

T_d : direct transmission probability

$$0 < T_d < i$$

Series QPCs

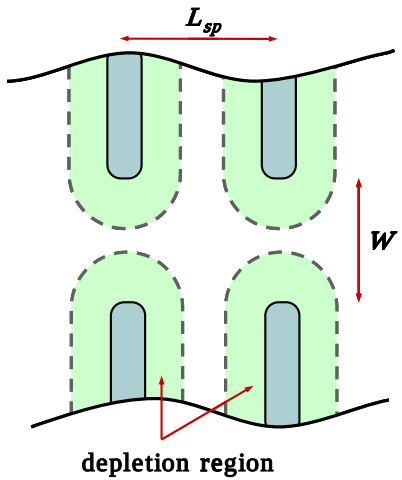

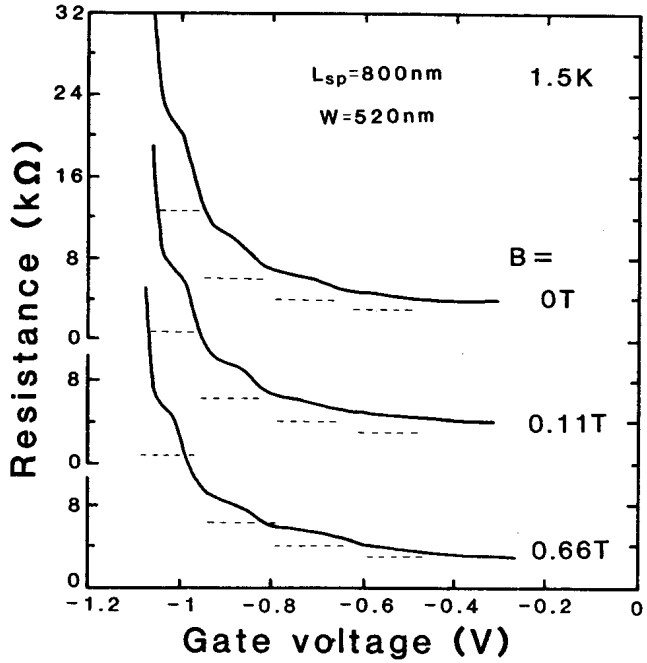

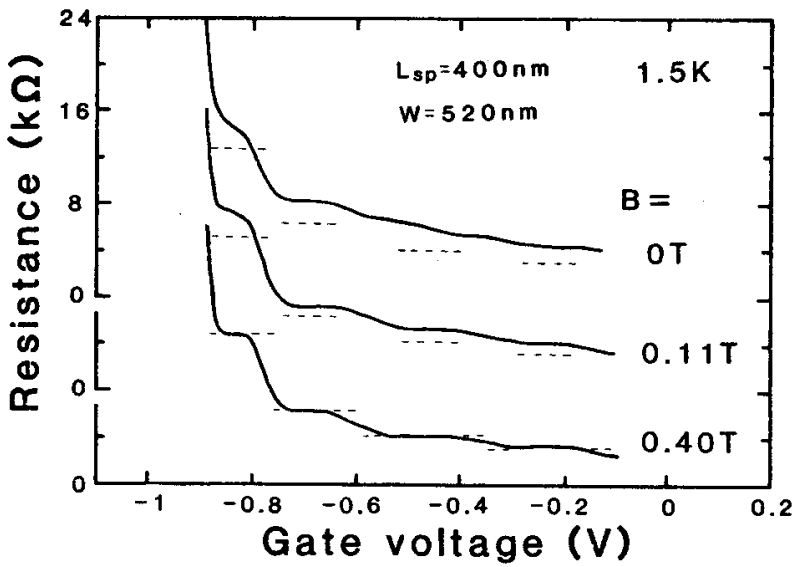

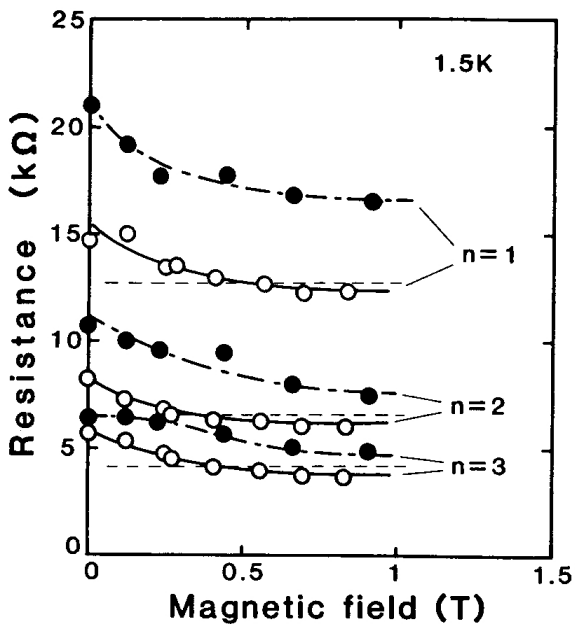

Y. Hirayama and T. Saku , Phys. Rev. B41, 2927 (1990)

Series QPCs

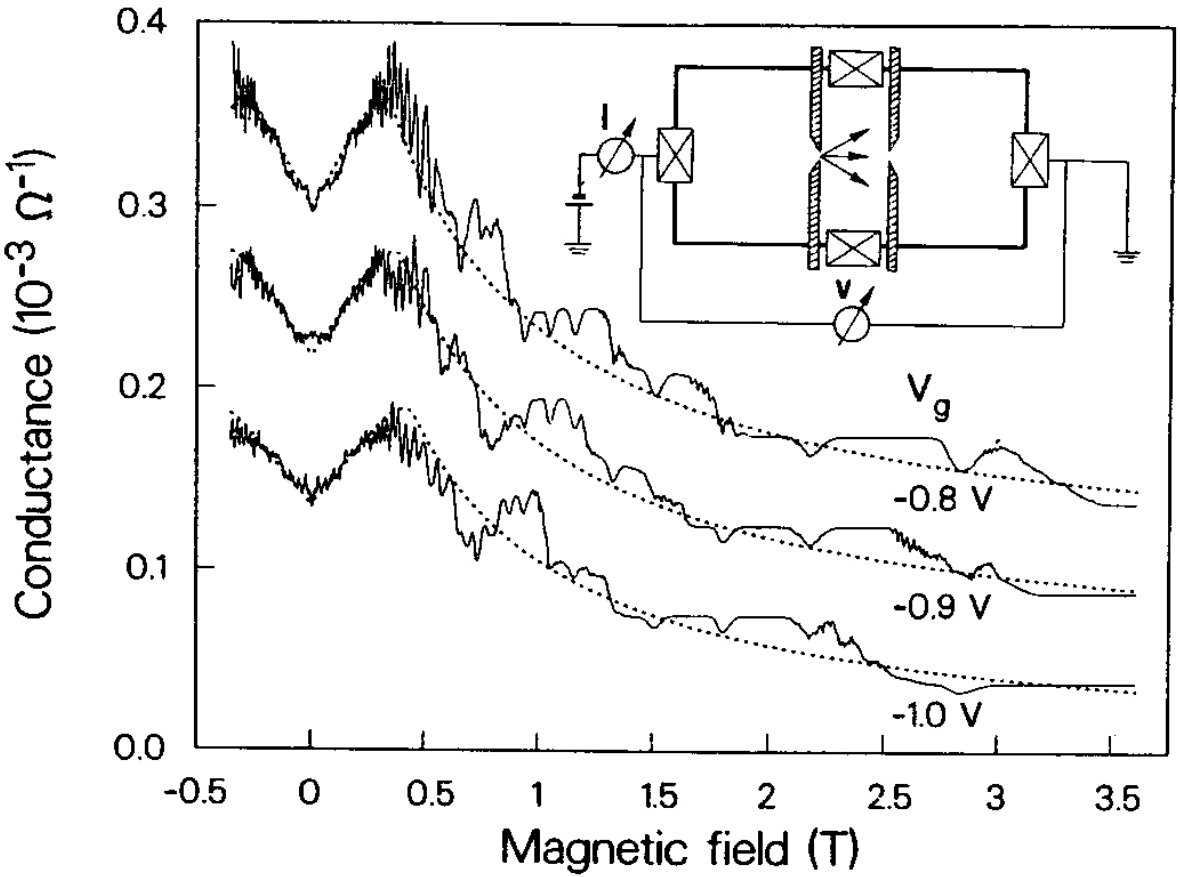

A. A. M. Staring *et al.*, Phys. Rev. B41, 8461 (1990)

Multiple parallel QPCs

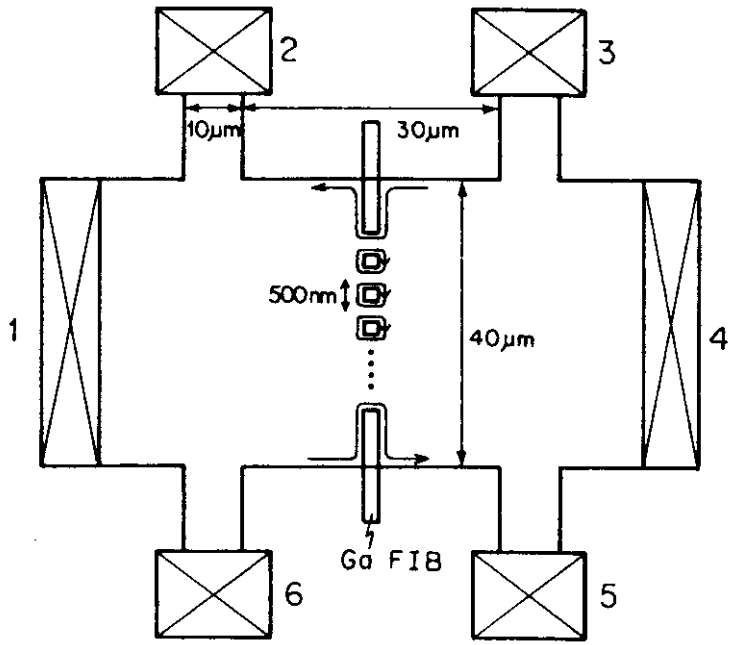

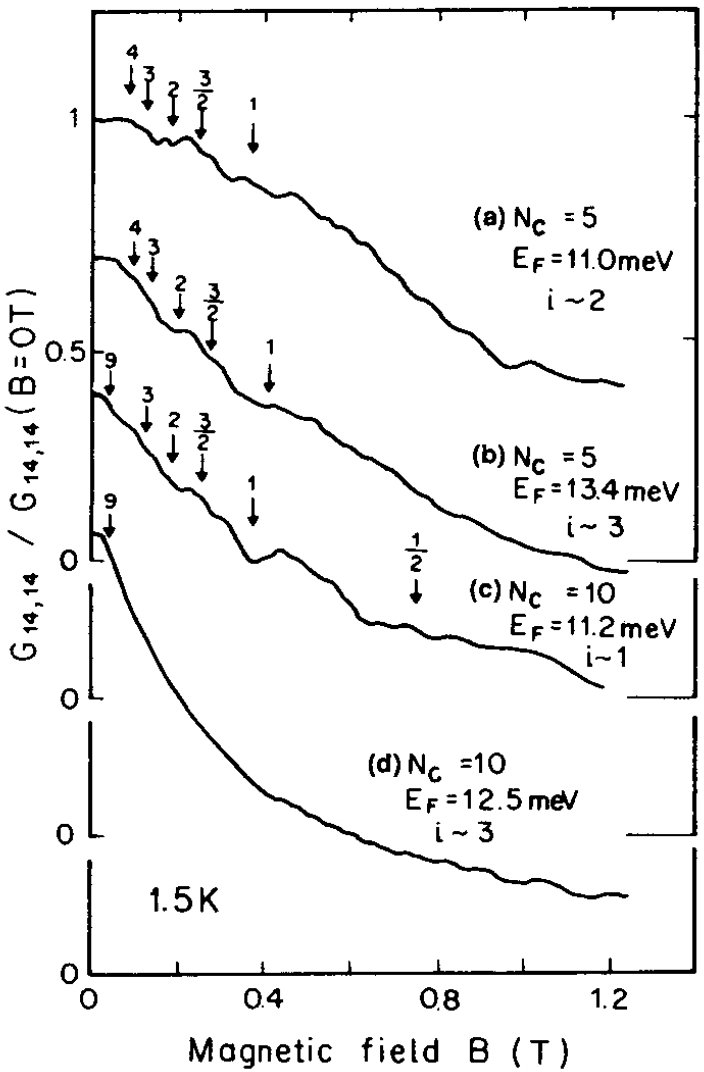

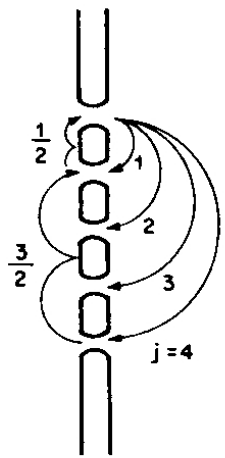

Large magneto-depopulation

Y. Hirayama and T. Saku, Phys. Rev. B42, 11408 (1990)

K. Nakamura *et al.*, Appl. Phys. Lett. 56, 385 (1990)

Multiple parallel QPCs

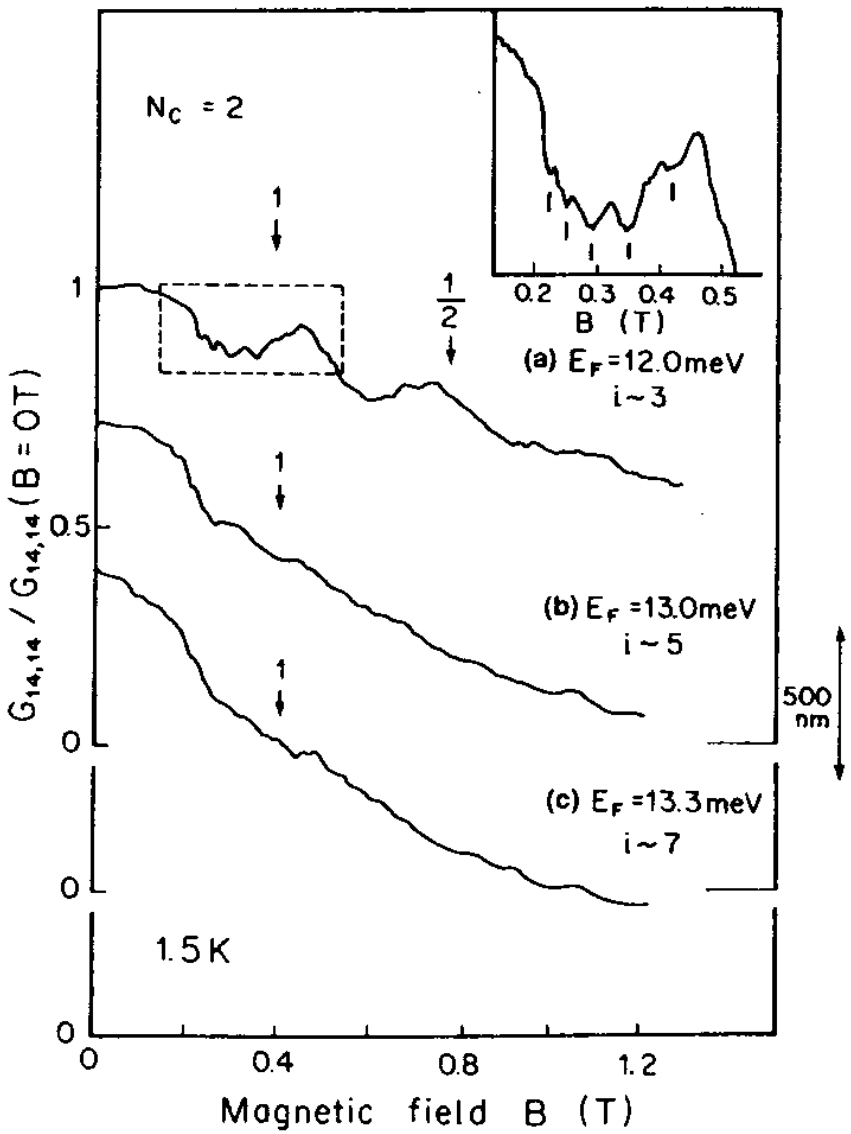

AB-type interference effect

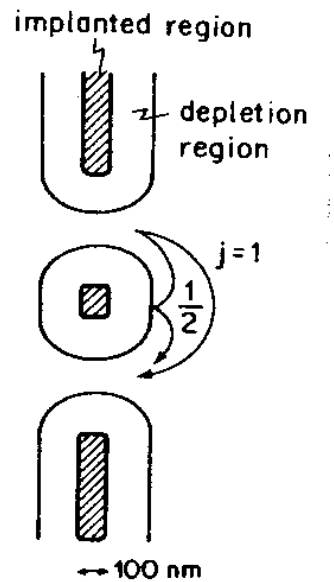

Y. Hirayama and T. Saku, Phys. Rev. B42, 11408 (1990)

Backgated heterostructure

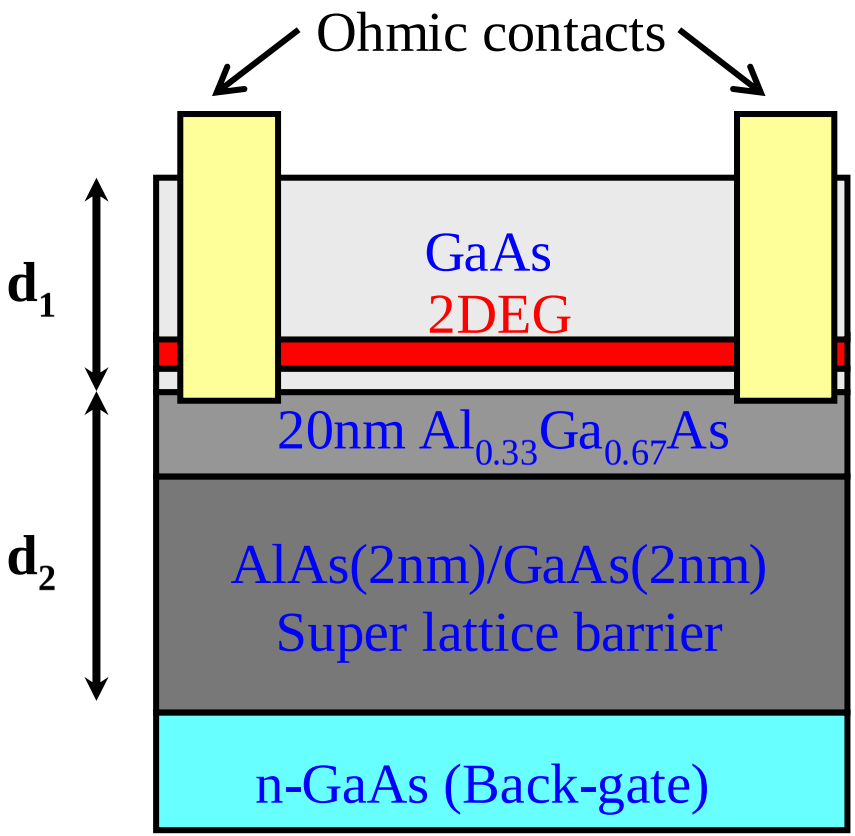

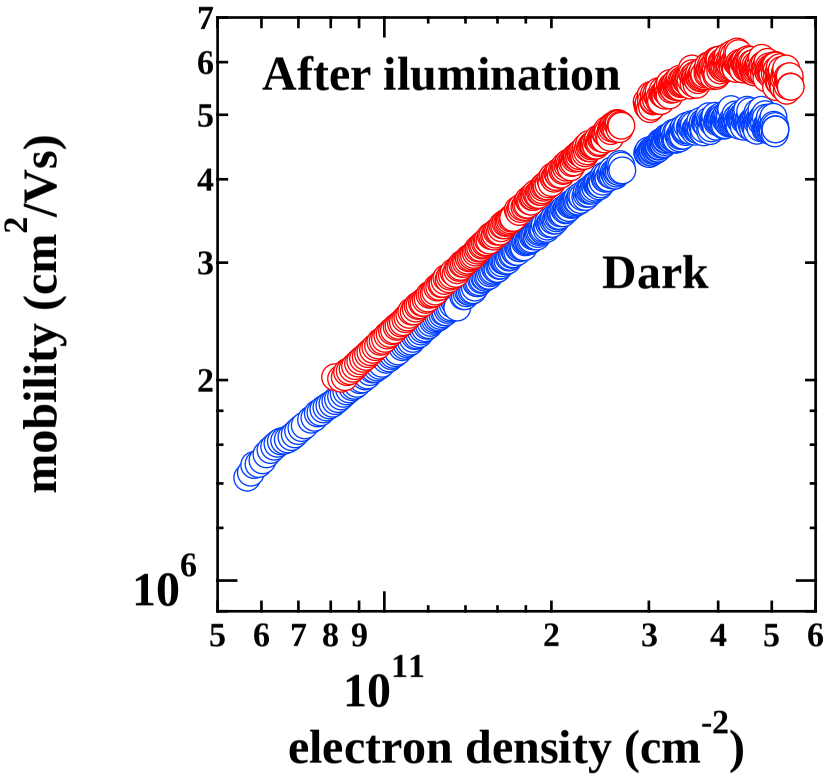

***d_1* (channel depth) : 54-500 nm**
***d_2* (barrier thickness) : 375-820 nm**

grown by MBE

Y. Hirayama et al., Appl. Phys. Lett. 72, 1745 (1998)

- Density tunability
- High mobility
- Appropriate system to study the surface characteristics

Characteristics of free GaAs surface
----- midgap pinning model (MPM) ------

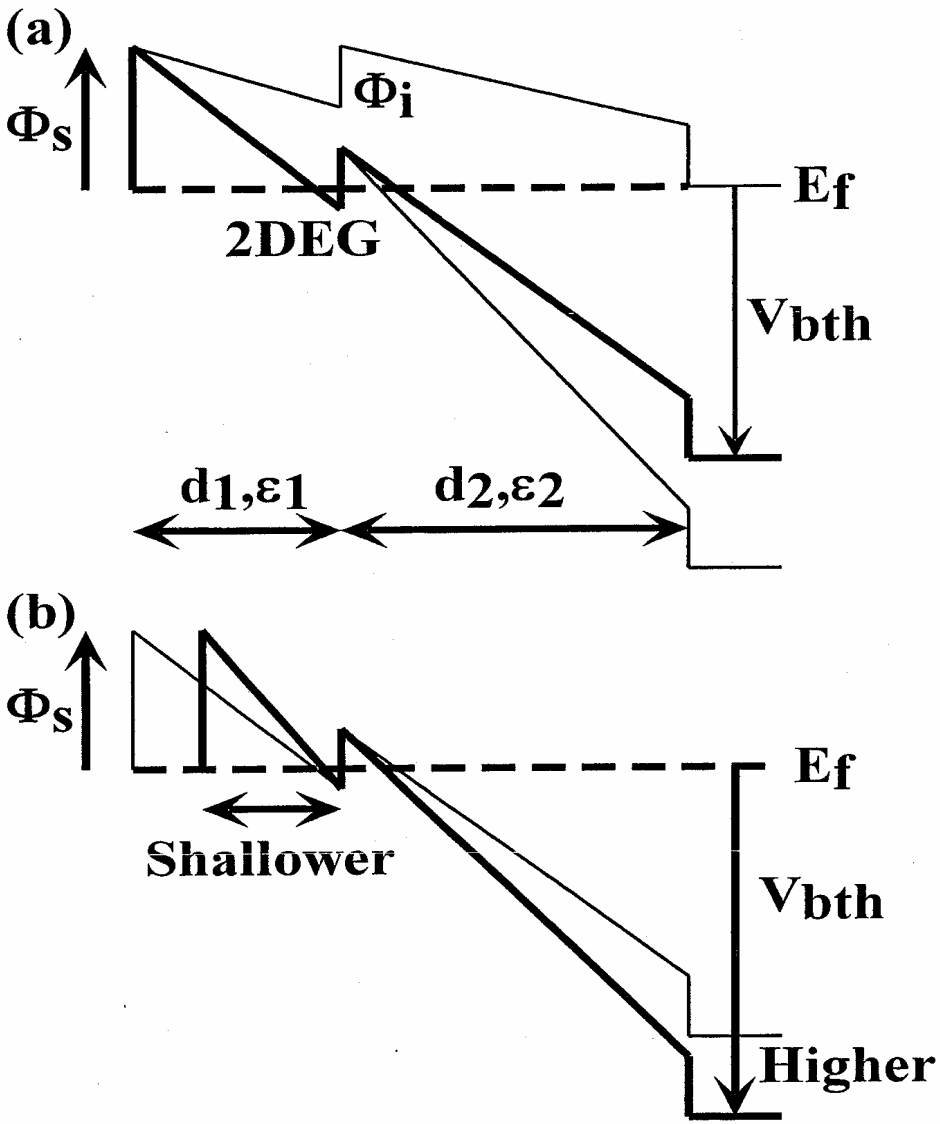

High quality

---> neglect impurity charge in GaAs

V_{bth} is determined by a balance of surface charge, 2DEG and backgate.

$$V_{bth} = \frac{d_2}{d_1}\frac{\varepsilon_1}{\varepsilon_2}\phi_s$$

$$\phi_s \approx mid-gap \approx 0.7 \sim 0.9eV$$

$$n = \frac{\varepsilon_2}{d_2 e}\left(V_b - V_{bth}\right)\left(V_b > V_{bth}\right)$$

Characteristics of free GaAs surface
----- frozen surface model (FSM) ------

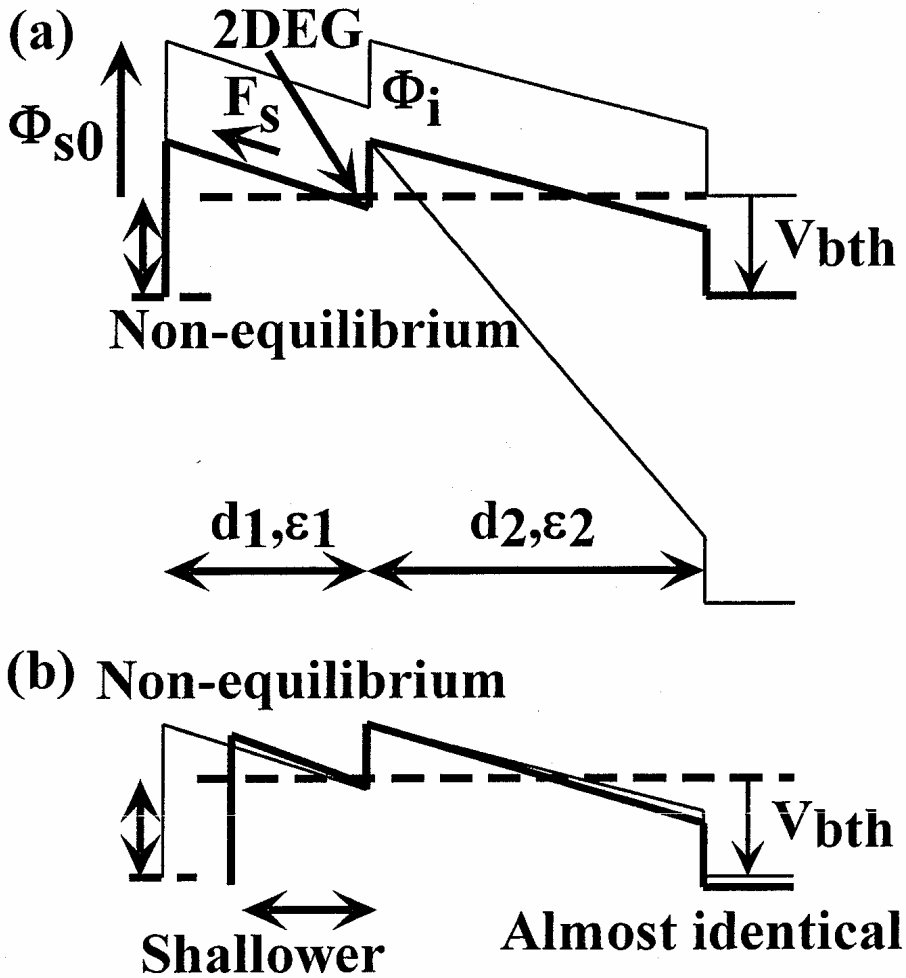

non-equilibrium surface

$$V_{bth} = \frac{d_2}{\varepsilon_2} Q_s$$

Q_s : *frozens surface charge density*

$$\phi_s = \left(\frac{d_1}{\varepsilon_1} + \frac{d_2}{\varepsilon_2} \right) Q_s$$

equilibrium before cooling

ϕ_s: *mid – gap*

$$\therefore \quad V_{bth} = \frac{d_2}{d_2 + (\varepsilon_2 / \varepsilon_1) d_1} \phi_s$$

$$n = \frac{\varepsilon_2}{d_2 e} (V_b - V_{bth}) \quad (V_b > V_{bth})$$

Threshold backgate bias of backgated undoped heterostructures

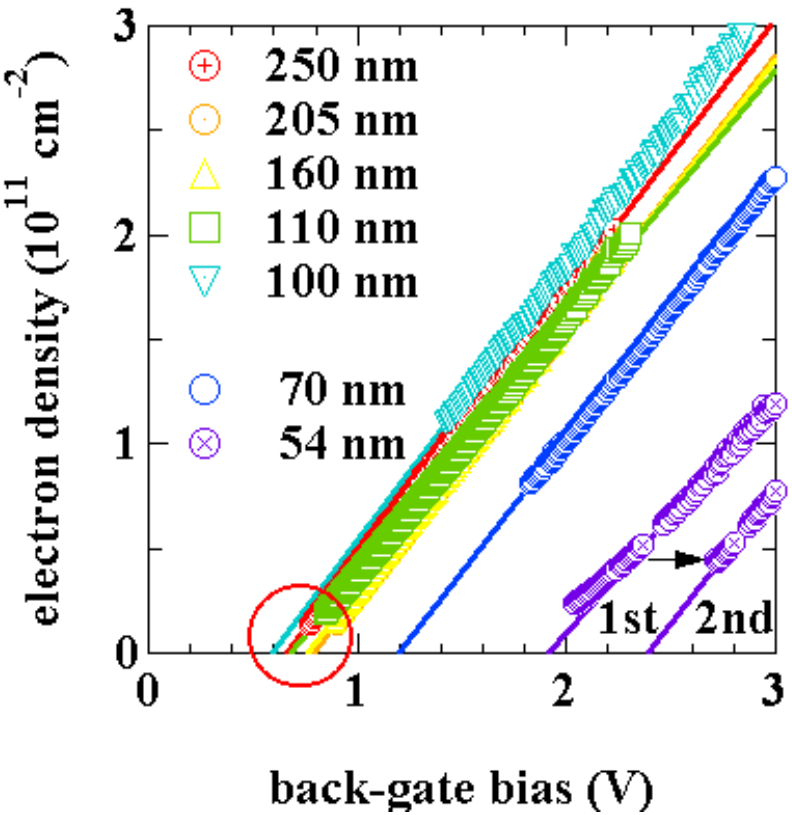

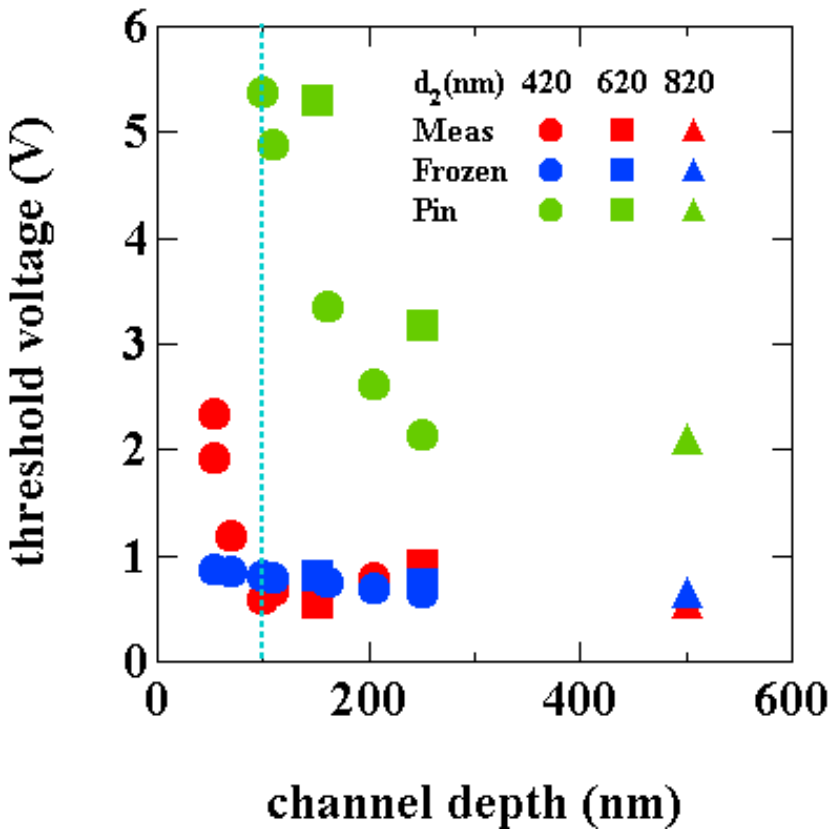

The obtained results are well explained by the frozen-surface-model.

A. Kawaharazuka et al., Phys. Rev. B63, 245309 (2001)

Shift of the threshold backgate bias

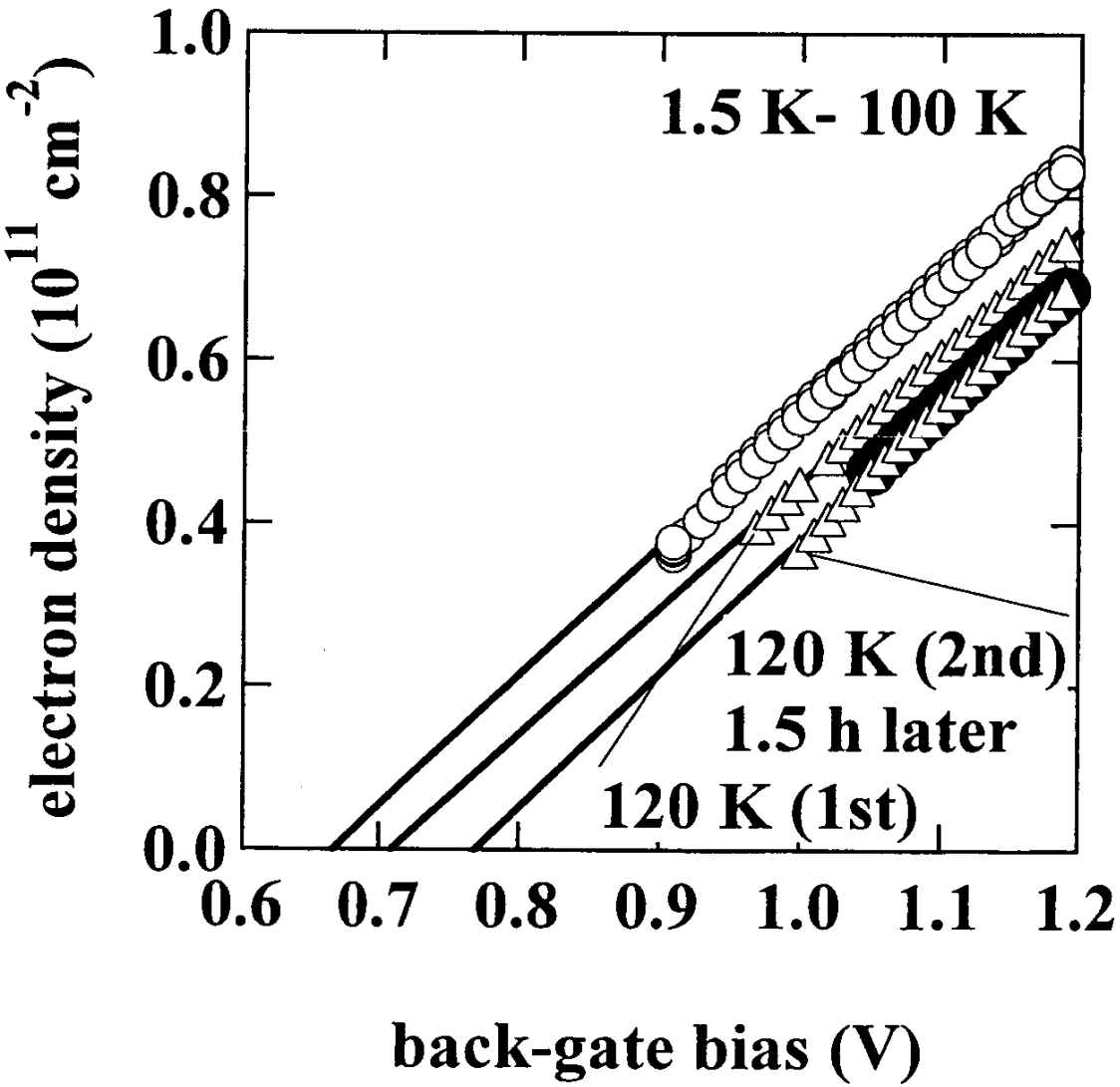

Charge transfer (electron tunneling to the surface) is observed at higher temperatures.

d_1 = 220 nm

A. Kawaharazuka et al., Phys. Rev. B63, 245309 (2001)

Erasable electron lithography

by using low-temperature scanning nanoprobe

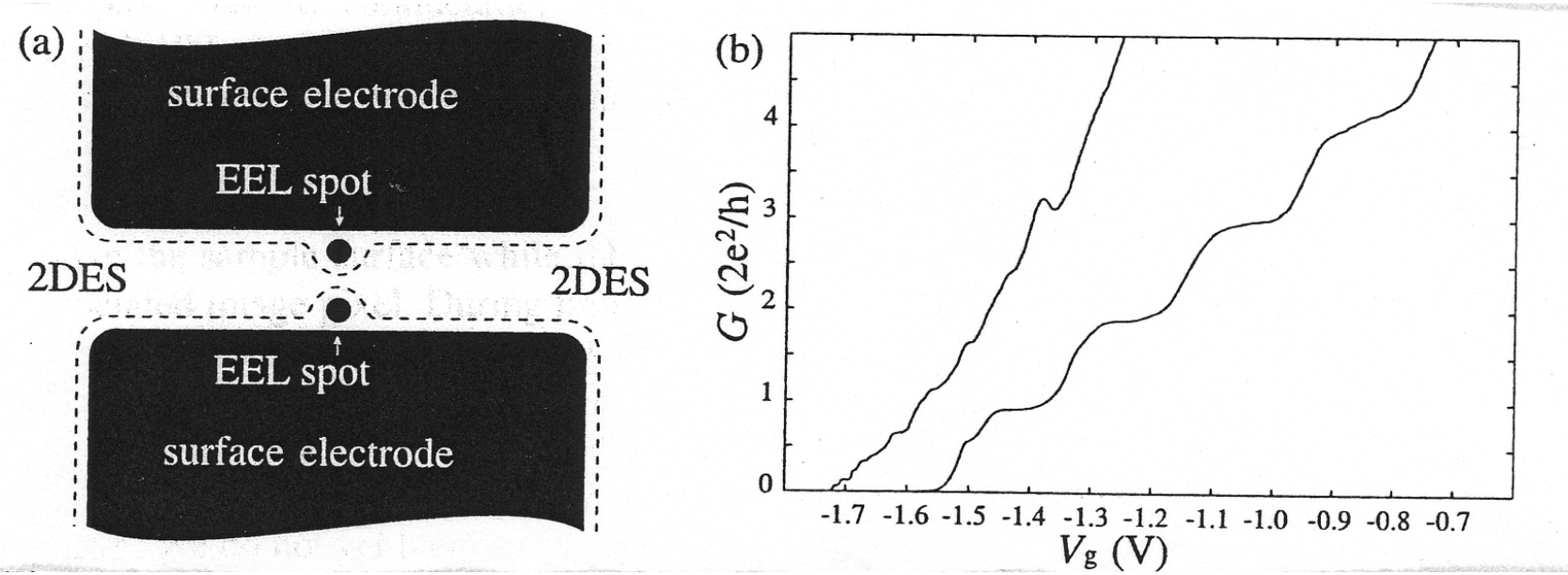

R. Crook et al., presented EP2DS-15 (Nara, 2003) H3

Electron flow through QPCs

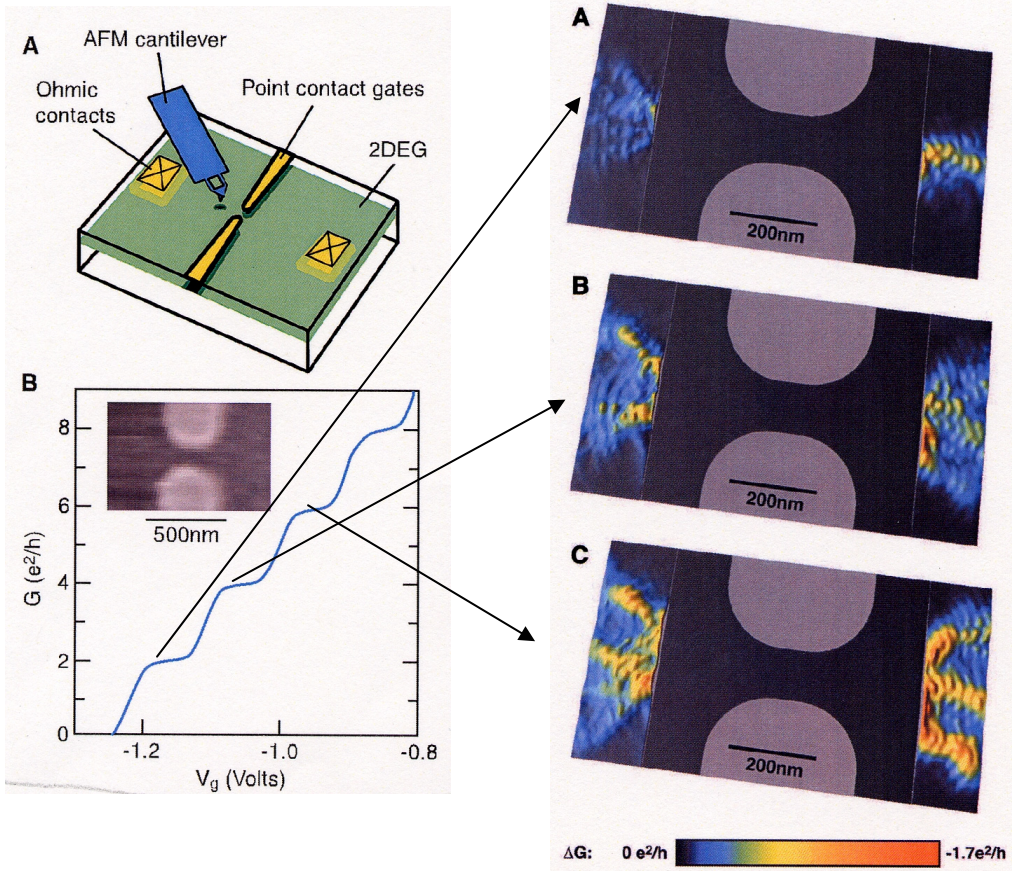

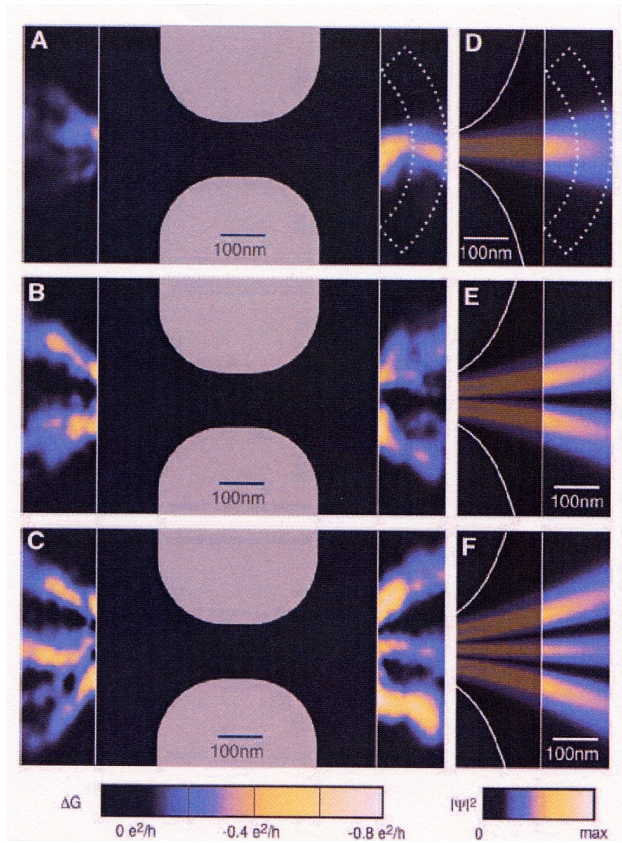

M. A. Topinka *et al.*, Science, 289, 2323 (2000)

Artificial point defect and deviation of the quatized conductance

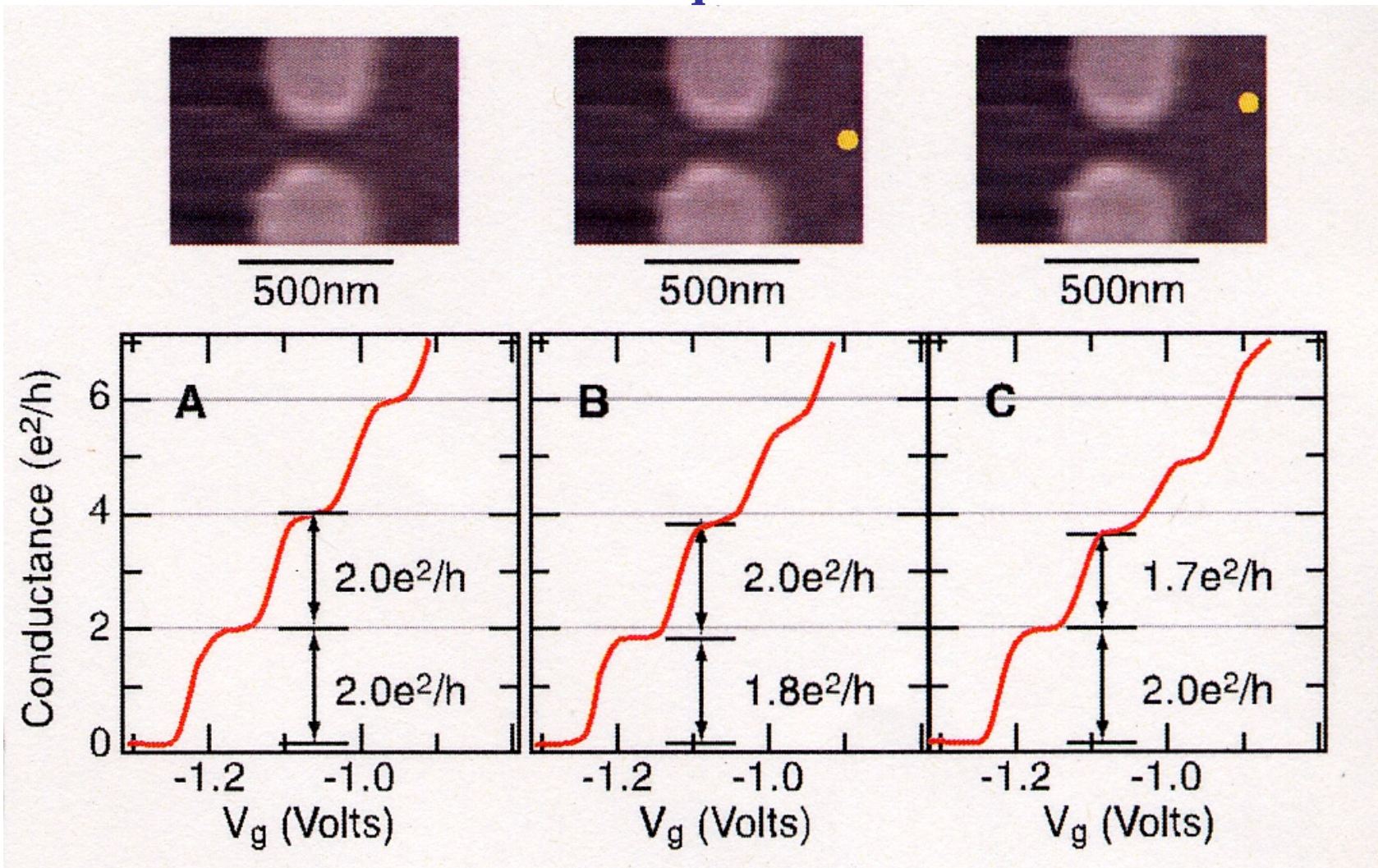

M. A. Topinka *et al*., Science, 289, 2323 (2000)

Electron flow pathes in real 2DEG (high-quality)

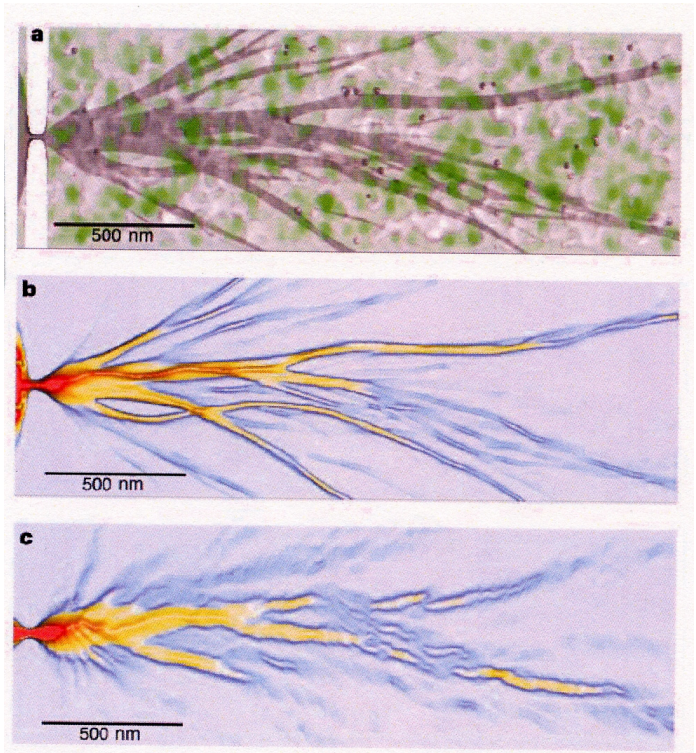

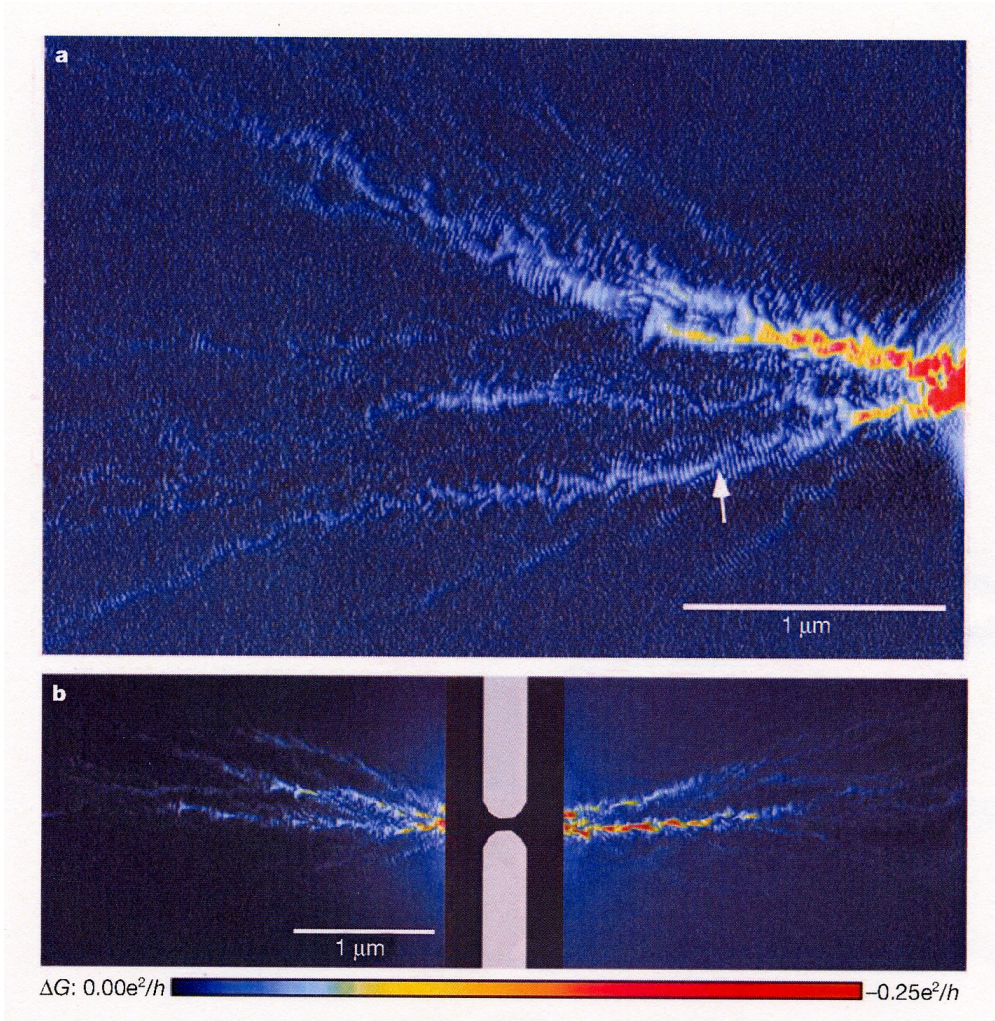

M. A. Topinka *et al*., Nature, 410, 183 (2001)

Quantum Point Contacts (QPCs)

I discussed principle characteristics of QPCs and related phenomena.

Quantized conductance and other features are well explained by single particle picture (quantum effects and ballistic effects)

Future

Combination of QPCs and other nanostructures

Spin-splitting at zero magnetic field?

Carrier interaction ---- 0.7 feature entangled electrons?

NTT

FEMD
CREST